Parameter Optimization For Segmenting Structures In CT images

A thesis

Submitted towards the partial fulfillment of
the requirements of the degree of

Master of Engineering
in
Electronic Instrumentation and Control Engineering

Submitted By:

Manjit verma
Roll No-80651011

Under the Esteemed guidance of:

Mr. M.D. Singh
Senior Lecturer

DEPARTMENT OF ELECTRICAL AND INSTRUMENTATION ENGINEERING
THAPAR UNIVERSITY
PATIALA – 147004

July - 2008

CERTIFICATE

*This is to certify that my work presented in this thesis entitled "**Parameter optimization for segmenting structures in CT images**" submitted in partial fulfillment of the requirement for the award of the degree of **Master of Engineering in Electronic Instrumentation and Control Engineering** at **Thapar University, Patiala**, is an original record under supervision and guidance of **Mr. M.D. Singh.** The matter embodied in this report has not been submitted anywhere for the award of any degree.*

Date: ***Manjit Verma***

Roll No - 80651011

It is certified that the above statement made by the student is correct to the best of our knowledge and belief.

(Mr. M.D. Singh)
Senior Lecturer, EIED
(Supervisor)
Thapar University, Patiala

(Dr. Smarajit Ghosh)
Professor & Head, EIED
Thapar University, Patiala

(Dr. R. K. Sharma)
Dean of Academic Affairs
Thapar University, Patiala

ACKNOWLEDGEMENT

Though it may appear that the following exposition is a monotonous beat of an unusual acknowledgement, I assert beyond the confines of the simple sense of word GRATITUDE. I take it as a highly esteemed privilege in expressing my sincere gratitude to my thesis supervisor Mr. M. D. Singh, Senior Lecturer in Electrical & Instrumentation Engineering Department for his kind and consistent guidance, encouragement and critical appraisal of the manuscript during the course of this thesis.

I am grateful to Dr. Smarajit Ghosh, Professor and Head of Electrical & Instrumentation Engineering Department for giving me, an encouragement and providing me his kind co-operation in enriching me in various roles and providing me all necessary facilities to work in the lab.

I am also grateful to Dr. R. K. Sharma, Dean of Academic Affair for his constant encouragement that was of great importance in the completion of the thesis.

I extend my thanks to Dr. Abhijit Mukherjee, Director, Thapar University for his valuable support that made me consistent performer.

I am also grateful to Dr. N. K Kandelwal, Head of Radiology Department, P.G.I for providing me the real images for test my code and verification of results.

This acknowledgement would be incomplete if I do not mention the emotional support and blessings provided by my friends especially Mr. Praveen Kumar for his kind co-operation.

Manjit verma

ABSTRACT

Medical imaging plays an important role in the diagnosis, therapy and treatment of various organs, tumors and other abnormalities. It benefits the patient through more rapid and precise disease management with lesser side effects. Segmentation in medical imaging provides an important role for calculating the geometric shape and size of tumors and abnormal growth of any tissue. Automatic segmentation in medical imaging is the challenging job for the researchers. It automatically calculates the exact values of place, position and area of the tumor or structural part of the image, which is needed for surgery and other treatments. There are many techniques available for auto-segmentation of images like Active contours, Fuzzy based classifiers, Gradient Vector Field theory, Tensor based segmentation, Level set theory etc. But many of them are suffering from problems like optimization, initialization and insufficient results in noisy images.

In this thesis we tried to optimize the Level set based segmentation process for different images on the basis of the texture analysis. In traditional methods, one has to select each parameter one by one to get best result and thus optimization is manually for every new image. However all the images have differed features like energy, entropy and contrast etc and these features are vary image to image (even within one image for its different parts). We tried to correlate the segmentation according to the texture features of an image, to make it automatic (no initialization of parameters) and more efficient

TABLE OF CONTENTS

LIST OF FIGURES

LIST OF TABLES

LIST OF ABBRIVATIONS

TIFF	Tagged Image File Format
PNG	Portable Network Graphics
GIF	Graphics Interchange Format
JPG	Joint Photographic Experts Group
BMP	Bitmap
DIB	Device-independent bitmap
CT	Computed Tomography
MRI	Magnetic Resonance Imaging
PDE	Partial Differential Equation
GLCM	Gray-Level Co-Occurrence Matrix
RGB	Red Green Blue
GVF	Gradient Vector Flow
GGVF	Generalized Gradient Vector Flow
CSAC	Cubic Spline Active Contour
MGVF	Motion Gradient Vector Flow

CHAPTER 1

INTRODUCTION

1.1 Overview

In the past four decades, computerized image segmentation has played an important role in medical imaging. Segmented images are now used in different applications, such as the quantification of tissue volumes, diagnosis, localization of pathology, study of anatomical structure, treatment planning, partial volume correction of functional imaging data, and computer-integrated surgery. Image segmentation remains a difficult task, due to both the tremendous variability of object shapes and the variation in image quality. In particular, medical images are often corrupted by noise, which can cause considerable difficulties when applying classical segmentation techniques. As a result, these techniques either fail completely or require some kind of post processing step to remove invalid object boundaries in the segmentation results. And problem is to tuning or optimized the segmentation methods by changing its topology.

To address this difficulty is used texture analysis for analysis the medical images so that one topology is define for one type of image and different topologies are store in one database. So program will choose its topology and change it automatically according to the image which is used to segmentation. First chapter introduce segmentation and its various types, after that texture analysis. Third chapter explain briefly about the methods which are used in thesis. And in chapter fourth and fifth is about the modified program and the results the program.

1.2 Segmentation

Segmentation refers to the process of partitioning a digital image into multiple regions (sets of pixels). The goal of segmentation is to simplify and change the representation of an image into something that is more meaningful and easier to analyze. Image segmentation is typically used to locate objects and boundaries (lines, curves, etc.) in images. The result of image segmentation is a set of regions that collectively cover the entire image, or a set of contours extracted from the image. Each of the pixels in a region are similar with respect to some characteristic or computed property, such as color, intensity, or texture. Adjacent regions are significantly different with respect to the same characteristic.

Some of the practical applications of medical image segmentation are:

- Locate tumors and other pathologies
- Measure tissue volumes
- Computer-guided surgery
- Diagnosis
- Treatment planning
- Study of anatomical structure

Some other applications are:

- Locate objects in satellite images (roads, forests, etc.)
- Face recognition
- Fingerprint recognition
- Automatic traffic controlling systems
- Machine vision

1.2.1 Methods

Several general-purpose algorithms and techniques have been developed for image segmentation. These are list below:

- Clustering methods
- Histogram-based methods

- Edge detection methods
- Region growing methods
- Level set methods
- Graph partitioning methods
- Watershed transformation
- Model based segmentation
- Semi-automatic segmentation
- Neural networks segmentation

1.3 Frequently used methods for segmentation

Several different segmentation techniques could be used to come up with similar results. The methods typically vary in speed, accuracy and robustness. Rather than trying to come up with yet another segmentation algorithm I wanted to select a few promising methods for comparison. In the following sections we will look into these three segmentation methods:

- **Snakes**
- **Level set**
- **Watershed**

1.3.1 Snakes, an active contour

In contrast to segmenting by thresholding or edge detectors a contour will have an elasticity that is adjusted to the actual application. We can think of an active contour as a snake that bends its body into the edge of the object. An important property of an active

contour is the ability to make continuous edges where the edges are weaker. Even if the edge is weak or broken we can make a continuous contour. The contour is described as a parametric curvature $v(s) = [x(s); y(s)]$ in a Cartesian xy-coordinate system where s is a parameter in the interval $[0; 1]$. Usually $v(s)$ is a spline. A snake is a special case of a more general technique to make a model fit into an object with use of energy minimization. The energy equation is given by the integral.

$$E^*_{snake} = \int_0^1 \{ E_{int}(v(s)) + E_{image}(v(s)) + E_{con}(v(s)) \}\, ds \quad \ldots\ldots\ldots\ldots\ldots\ldots\ldots\ldots\ldots\ldots (1)$$

Where E_{int} is the energy in the spline, E_{image} comes from forces in the image and E_{con} from external constraint forces. The last two are energy from outside forces. The internal energy can be described with a differential equation where the first and second differentiate of the curve v describes stretch and stiffness in the spline. If we use the analogy with the snake it is expandable like a rubber band and works against bending.

1.3.2 Level set segmentation

Segmenting images with level set methods was introduced at the end of the 1980's and was based on previous work on moving curvatures. Since then several variants and improvements have come up. Some of the improvements are aimed at speeding up the processing. Other methods have strength related to specific challenges like noise and broken edges.

In the level set method, the curve is represented implicitly as a level set of a 2D scalar function referred to as the level set function which is usually defined on the same domain as the image. The level set is defined as the set of points that have the same function value. Fig1.4 shows an example of embedding a curve as a zero level set. It is worth noting that the level set function is different from the level sets of images, which are sometimes used for image enhancement. The sole purpose of the level set function is to provide an implicit representation of the evolving curve.

Instead of tracking a curve through time, the level set method evolves a curve by updating the level set function at fixed coordinates through time. This perspective is similar to that of an Eulerian formulation of motion as opposed to a Lagrangian formulation, which is analogous to the parametric deformable model. A useful property of this approach is that the level set function remains a valid function while the embedded curve can change its topology. This situation is depicted in Fig 1.4 and 1.5. [35]

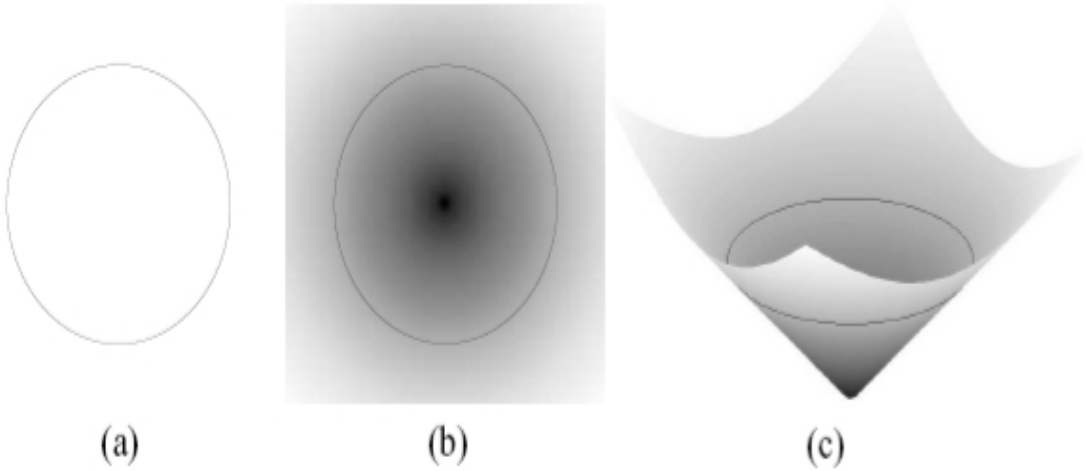

Fig 1.1: An example of embedding a curve as a level set. ((a) A single curve. (b) The level set function where the curve is embedded as the zero level set (in black). (c) The height map of the level set function with its zero level set depicted in black)

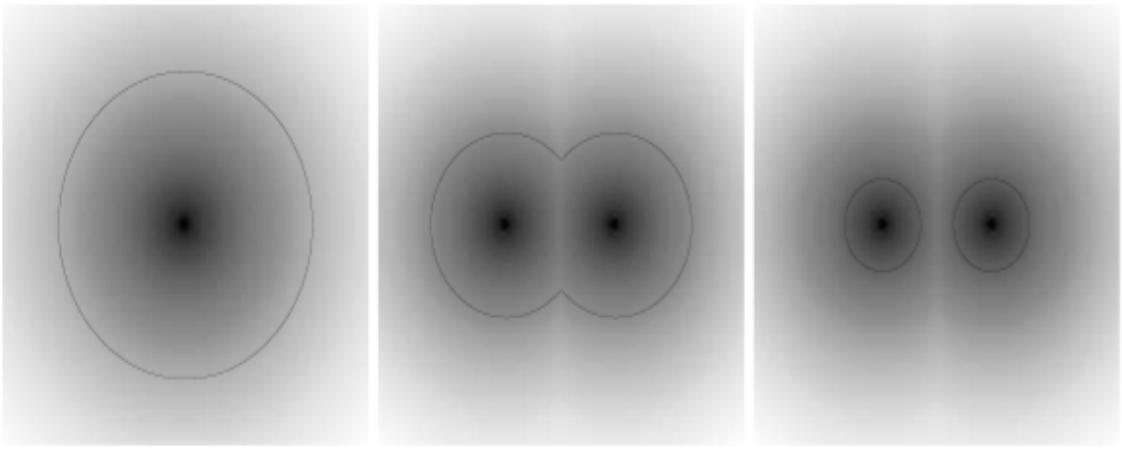

Fig 1.2: Zero level set for single and double curves(From left to right, the zero level set splits into two curves while the level set function still remain a valid function)

1.3.3 Watershed segmentation

Watershed segmentation uses the analogy from topography. By interpreting the gradient map of an intensity image as height values we get lines which appear to be ridges. If the contours were a terrain, falling rain would find the way from the dividing lines towards the connected catchments basin. These dividing lines are called watersheds. fig 1.6 [35] illustrates that steep edges cause high gradients which are watersheds. The edge feature map is not limited to gradient magnitude. Other measures such as texture and intensity can be combined to get the best possible separation of the classes. The homogeneous areas of the image cause low edge feature values and forms the catchments basins. There might be an idea to truncate values below a given threshold to reduce the number of regions detected.

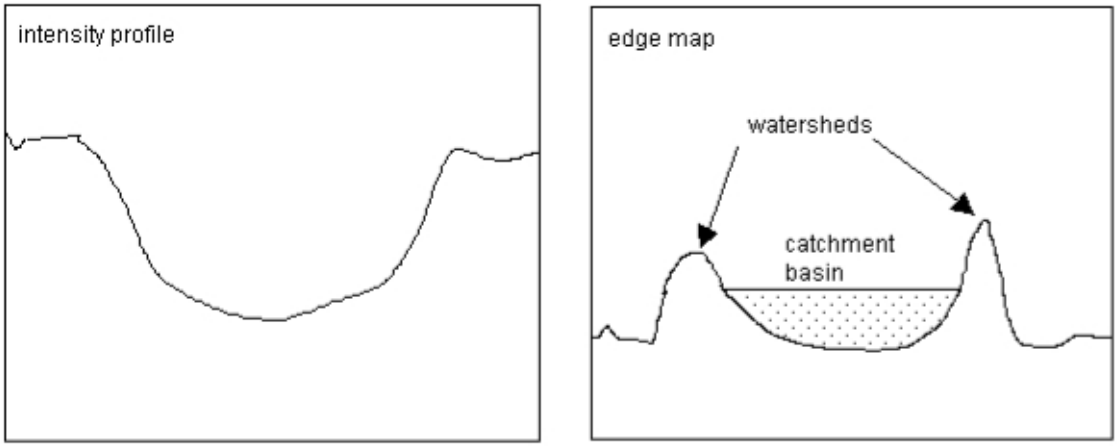

Fig 1.3: Watershed segmentation simplified to one dimension

1.4 Texture analysis

Texture is used to describe two dimensional arrays of variation. The elements and rules of spacing or arrangement in texture may be arbitrarily manipulated, provided a characteristic repetitiveness remains. This texture analysis I used for getting the feature from the image. Their different types of methods for calculating the texture analysis. They are described below:

- **Statistical** methods analyze the spatial distribution of gray values, by computing local features at each point in the image, and deriving a set of statistics from the distributions of the local features. Depending on the number of pixels defining the local feature statistical methods can be further classified into first-order (one pixel), second-order (two pixels) and higher-order (three or more pixels) statistics. This method I used in my thesis and explain briefly in chapter 3

- **Geometrical** is characterized by their definition of texture as being composed of "texture elements" or primitives. The method of analysis usually depends upon

the geometric properties of these texture elements. First of all we have to calculate these primitives. After this extract the placement rule that describes the texture.

- **Model Based method is** based on the construction of an image model that can be used not only to describe texture, but also to synthesize it. The model parameters capture the essential perceived qualities of texture.

- **Signal Processing Methods** analyze the frequency content of the image. partial domain filters are used in this method.

CHAPTER 2

RELATED WORK

Chris Davatzikos and Jerry L. Prince in 1993 presented two adaptive active contour algorithms that reconstruct the nearly constant speed parameterization of the skeleton of a thick curve. They are based on a time and partially varying regularization constant respectively. The algorithm was good for thick curves. The parameter K_O determines the elasticity of the active contour and is of major importance in this Paper.

Thick curves arise naturally in certain applications such as MRI of brain. In this type of image simple active contour not give results because of lack of conditions under which they yield good solutions. In first they presented a new active contour model for thick curves and derived conditions under which it gives a good solution. In second the external forces of this model are based on a local averaging rather than differentiation, making the proposed method more robust to noise and discrimination errors. The performance of the time-adaptive algorithm is impressive; its computations are time consuming since K_O sweeps a very large interval before it eventually assumes its final value. The spatially adaptive algorithm was shown to be a good compromise between the non-adaptive and the time-adaptive algorithms. Although the way that the regularization parameter K_O is varied in these two formulations is somewhat heuristic, the results are promising. [1]

C.T. Tsai et al. in1993 used Hopfield Network for minimizing the energy in contour model and testing on medical images. An active contour model (snake) is a closed spline curve whose deformation is driven by the internal, the image, and the external forces. a parametric representation of an active contour $V(s) = (X(s), Y(s))$, the energy function can be written as:

$$E_{snake} = \int_0^1 E_{snake}(V(s))\, ds$$

$$= \int_0^1 E_{int}(V(s)) + E_{img}(V(s)) + E_{con}(V(s))\, ds.$$

E_{int}, here represents the internal force of the contour due to bending or discontinuities, E_{img} is the image force, and E_{con} is the external force. The image forces are generated by various events, for example lines, edges, and terminations. The external force describes the high-level knowledge about the contour of objects and is always define by the user. It can be included in the energy model of snakes when the high-level constraint is necessary to define the object contour. The Hopfield neural network, due to its simple architecture and well-defined time behavior, has been used in various applications. State evolutions of this network are based on decreasing the energy function. Hence, it is inherently suitable for solving optimization problems. Because *of* its intrinsic characteristics, this type of network is well suited to our applications for solving the energy minimization problems of active contour models. [2]

D.N. Davis et al in 1994 gave the basic idea about active contours used for CT and MRI images. Active contour models (or snakes) are a special form of deformable models, characterized by their property of dynamic deformation to an image from an original given shape. This deformation is controlled through the minimization of an energy function. The algorithm is based on property of deformation model that is controlled through the minimization of an energy function.

Magnetic Resonance Imaging (MRI) and Computed Tomography (CT) are two very different methods for producing three-dimensional radiological image data sets. CT is a digital radiological technique using low dose X-rays which allows some degree of flexibility in use to control and manipulate the formation and presentation of images. MRI is different than CT; in that X-ray radiation is not used, but relies on very high magnetic fields and radio-frequency of a specific wavelength.

The snake is defined as an energy minimizing spline; with its energy dependent upon its shape and local image characteristics. Typically, local energy minima correspond to desired image properties. The energy function to be minimized is a weighted combination of internal and external energy forces. Snakes bend themselves to object delineation, particularly where guided by higher level understanding processes. They require a starting shape and location, preferably near to that of the desired object. The internal energy at any given node is combination of forces controlling elasticity and stiffness, and tends to produce smooth contours. [3]

M. Xiao et al. 1994 proposed the research result on contour extraction from high voltage electron microscope (HVEM) images of thick cross section montages of small blood vessels.

In real-world images especially medical images, object boundaries arc usually hard to be detected solely on the basis of their photometry because of the presence of noise and various photometry anomalies. Thus, all methods for finding boundaries based on purely local statistical criteria are bounded to generate errors, finding either too many or too few edges, because they lack a geometrical model to guide their search. Based on these problems, a technique arises that integrates both photometry and geometric models with an initial estimate of the boundary. The models are incorporated by defining an energy function for curves that is minimal when the models are maximally satisfied. The initial estimate is used as the starting points for finding a local minimum of this energy function. The strength of this energy-minimizing curve approach is that the geometry constraints are directly used to guide the search for a boundary and that the edge information is integrated along the entire length of the curve, thereby providing a large support without including the irrelevant information off of the cum and at the same time finding boundaries that could not otherwise be found. This kind of geometric model is what are called active contour models.[4]

Guillermo Sapiro 1996 presented geometric active contours detected edges in vector valued image. The techniques are applicable for example to color and texture images.

The image processing algorithm uses are image processing algorithms as anisotropic diffusion and shock filters. It gives better approach in segmentation of images. One of the basic problems in image analysis is object segmentation. Object detection and image segmentation has been studied since the early days of computer vision and image processing, and different approaches have been proposed. Object segmentation can be associated with the problem of boundary detection and integration, when boundary is roughly defined as a curve or surface separating homogeneous regions. The classical snakes approach is based on deforming an initial contour or surface towards the boundary of the object to be detected Vector-valued images are not just obtained in image modalities were the data is recorded in a vector fashion, as in color (RGB, luminance chrominance), medical (MRI, X-ray, ultrasound) and LANDSAT applications. The vector-valued data can be obtained also from scale and orientation decompositions very popular in texture analysis. In general, two different approaches can be adopted to work on vector-valued images. The first approach is to process each plane separately, with the geodesic active contours then integrate the results of this operation to obtain one unique segmentation for the whole image. The second approach is to integrate the vector information from the very beginning, and deform a unique curve based on this information, directly obtaining a unique object segmentation [5].

Tianyun Ma and Hemant D. Tagare 1999 proposed a new algorithm for making the contour stable at true edges .the minimization of energy is does not occur at the edges ,so it give new algorithm in which it is replaced single external energy function with sequence of energy functions. This algorithm we can use in any other algorithm because it is not for any specific application.

An active contour is an evolving curve that follows gradient dynamics until it is stationary at a minimum of a sum of external energy and internal energy. The external energy depends on the image and the internal energy depends on the active contour geometry. Euclidean arc length external energies are biased. That is, the minimum of the external energy of an edge-seeking active contour does not occur at the edge. This is not the effect of noise, but is the effect of using Euclidean arc length integrals in the energy

term. One solution to these problems is to use a non-Euclidean arc length for the contour. The arc length can be defined such that the length of an infinitesimal piece of the contour does not change when it is pushed in the normal direction. This leads to a different formulation of active contours where the contour evolves as an integral curve of a vector field which is the gradient of a local energy function. The active contour does not have a global energy function. These active contours are not biased [6].

F. Mendels et al. 1999 proposed a method which used level set and GVF methods of segmentation for retina images, both the method show fine result. Both the methods detected the boundaries of blood vessels without any distortion. The optic disk is a significant anatomical landmark in the retina. Various ophthalmic pathologies, especially glaucoma, are manifest by changes in the shape, pallor, or depth of the optic disk region. Accurate identification of the outer boundary of the optic disk may allow ophthalmologists to quantitatively assess changes in the optic disk over time. Initial formulations of active contours suffered from a need for good initialization, and an inability to move into small concavities. A gradient vector flow (GVF) based snake was introduced to address these limitations. In this formulation, a more general external force is defined which gives a directional field that accounts for boundary proximity, but with a larger range of attraction. This decreases the sensitivity to initial conditions. An alternative approach to boundary detection is offered by level-set theory. In this, a desired propagating boundary is considered as the zero level set of a higher dimensional function [7].

Yuki Matsuzawa and Toru Abe 1999 proposed another fast and accurate method for region extraction in the images. It give a new method which reflects wide-ranging region information to region extracting process through competition of active contours effectively used for extracting objects with complex image features or background, because they are deformed mainly based on the local image features along the contours which cannot be detected by conventional method. In the proposed method, firstly, set the initial curves in object and background then divide these curves into segments as

cores of initial contours. Secondly, estimate feature distribution inside of each contour, and determine the control points to each contour with respect to image features. Each contour performs region competition based on the likelihood. Finally an object is extracted as a set of multiple active contours [8].

Tony F. Chan and Luminita A. Vese 2001 proposed a new method of active contour without edges for detection of an object in an image, based on curve evolution. This method detects objects whose boundaries are not necessarily defined by gradient or with very smooth boundaries, for which the classical active contour models are not applicable. They used two approaches that are; Mumford–Shah functional for segmentation and level sets. The advantages are it doesn't required to smooth the initial image the locations of boundaries are very well detected and preserved and it is not based on an edge-function to stop the evolving curve on the desired boundary . This model can automatically detect interior contours starting with only one initial curve. The position of the initial curve can be anywhere in the image, and it does not necessarily surround the objects to be detected [9].

Nilanjan Ray et al. 2001 used simple GVF based parametric contour for segmentation .tested on lung images for measuring air spaces. There is nothing difference in algorithm rather than effectively overcome the overlapping of contours. The active contour approach is computationally inexpensive and is independent of initial contour placement as compared to traditional active contour. For classification of the functional lung air space in the helium images, a fuzzy c-means technique is applied. In this paper, they used a segmentation technique for determining total lung air space. The analysis depends upon the information from two modalities. First from Proton images, that reveal the lung cavity and Second from Helium images, showing the ventilated portions of the lungs. So for quantify the functional lung air space they compare the volume extracted from the proton imagery and the volume extracted from the helium imagery. The proposed method of diffusion is superior to the original GGVF. Other active contour methods such as the pressure force, the distance force and the GGVF (or GVF) are incapable of automatically

merging snakes. These methods allow the overlapping of snakes that collide in evolution. The proposed method closely resembles the pressure snake, except that it prevents overlapping. More importantly, the pressure snake suffers from a lack of control over stopping at weak edges. The proposed method overcomes this difficulty as well, since the underlying diffusion process is a GGVF [10].

Di Xiao et al. 2002 proposed multi-gradient contour for detection of multilayer boundary of ultrasound images. To extract useful information for clinical diagnosis, surgeons need to view ultrasound images slice by slice, which is still a time-consuming and tough work for physician to perform object recognition and information gathering. The main objective of this paper is to develop an image processing algorithm for anal anatomical structure detection from its Ultrasound image. The obtained boundary information about anal muscular layer can help physician to get the necessary information and determine therapeutic steps to treat the patients. This work will reduce the need for physician to mesh with large quantities and, time-consuming work on image analysis [11].

LJ Spreeuwers and M Breeuwer 2002 proposed a method of coupled active contour which give better result on low contrast and noisy medical images. This paper describes the simultaneous extraction of expand endocardial boundaries using a set of coupled active contours in MR short axis cine recordings. Manual tracing of the contours in all images is a rather time consuming task, therefore, methods were proposed to automatically or semi-automatically extract the contours from short axis images. Problems that complicate automatic contour are extraction are low contrast between the myocardium and other tissues and the papillary muscles, that for wall thickness measurements must be placed inside and for left ventricular volume measurements outside the endocardial boundary. Generally, the epi- and endocardial boundaries are treated independently and the two contours are extracted separately. In this paper a coupled active contour approach is proposed that exploits the fact that the epi- and endocardial boundaries are not independent and extracts both contours simultaneously [12].

Ning Xu et al. 2003 proposed new algorithm for active contour. It is a combination of active contours and the optimization tool of graph cuts which give ability to jump over local minima and provide a more global result and also give smooth contour. But drawback of our algorithm is that we must construct the graph with appropriate pixel connectivity and edge weights.

Many approaches have been proposed to improve the robustness and stability of Snakes. The active contours then are stopped by a strong edge but move past a spurious edge which is weak In contrast to the framework of active contours, graph cuts approaches are applied as global optimization methods for computer vision problems such as image segmentation The image is represented using an adjacency graph. Each vertex of the graph represents an image pixel, while the edge weight between two vertices represents the similarity between two corresponding pixels. The exact solution can be found in polynomial time A key assumption of this approach is that the desired segmentation contour is a global minimum within its size (width) contour neighborhood. It has the ability to jump over local minima and provide a more global result. Graph cuts guarantee continuity and lead to smooth contours free of self-crossing and uneven spacing problems.

Peter J. Yim and David J. Foran. 2003 proposed the segmentation of CT images with watershed and active contour method and proposed standard value of parameters which give better segmentation results. It compares both methods. The Watershed algorithm was ineffective since it produced gross segmentation errors on a majority of the lesion slices while the active contour with initialization by manual contouring produced no significant improvement in reproducibility. Tumor size is a primary measure of the severity of cancers. The conventional standard for measuring tumor size is a bi-dimensional measurement formalized by the World Health Organization. The use of volumetric measurements of tumor size is clearly a more universal standard and may prove to be more accurate than dimensional measurements for detecting changes in tumor size. The watershed algorithm and the active contour algorithm algorithms are

geometrical in nature and initialized by manual tracing. A multi-scale active contour algorithm initialized by ellipses. The algorithms are characterized by comparison with results from manual tracing alone and in terms of their reproducibility [14].

Lijun Yin et al. 2003 proposed an automatic detection of regions of interest (tumor areas) has long been demanded for the purpose of the medical diagnosis. The accurate estimation of the shape and area of the lesion can help doctors to assess the lesion status before and after the treatment. A number of methods have been proposed for tumor/ lesion region detection and segmentation, including multi-resolution segmentation, wavelet based detection, deformable model based energy minimization, texture segmentation, template and feature matching and neural network. Wavelet transform for multi-resolution segmentation uses M-channel wavelets at different resolution levels for better mass segmentation. Deformable model (e.g., active contour) is widely used in region detection and segmentation for medical image data. This active contour model can correctly localize the edges and contours given a good initial estimation. But the algorithm is prone to finding the false salient features or the noise. So this paper brings 'mesh based active contour method' which is very helpful in detection of location and shape of the object in initial stage. Intelligent mesh is an extension of the dynamic mesh based on the principle of the mesh energy minimization during the mesh converging to the feature regions of images. In the first stage, the intelligent mesh will distribute itself to the feature region by the nodes motion. The node distribution can signify the features of interest. In the second stage, the fine selection of the feature region will be carried out for screening the feature region from all the possible candidate regions which have been detected. The location and the size of all the feature regions can be initialized in this stage. In the last stage, the mesh energy will be used to guide the active contour model to extract the fine contour of the feature region [15].

Raquel Valdés and Cristerna. 2004 proposed a hybrid model for segmentation of MRI images of brain. The model couples a segmenter, based on a radial basis network (RBFNN), and an active contour model, based on a cubic spline active contour (CSAC)

interpolation. The active contour and surface models offer a powerful tool for medical image analysis by combining geometrical and physical constraints. In this paper, a hybrid methodology for brain multi-spectral MRI segmentation is proposed an adaptable scheme of the hybrid model and a re-sampling mechanism for the optimal selection of control points, are also presented [16].

Nilanjan Ray and Scott T. Acton. 2004 proposed a novel external force for tracking rolling leukocytes observed in intravital video microscopy. Existing active contour force models, such as GVF, MGVF utilized the direction of leukocyte movement. It show that while GVF is unsuitable for tracking fast rolling leukocytes, MGVF is well adapted to both fast and slow rolling. Equivalently, MGVF performs well when the temporal resolution of a leukocyte rolling sequence is reduced, and thus can be used to increase throughput [17].

M. Savelonas et al. 2005 proposed a novel active contour model named Variable Background Active Contour model. It applied for the detection of thyroid nodules in ultrasound images. This model has edge independency, no need for smoothing, ability for topological changes and it is more accurate when compared to the Active Contour without Edges model. This model uses a variable background to reduce the effects of image in homogeneities. The ultrasound images produced by this technique contain echo perturbations and speckle noise, which follows a Raleigh distribution that cannot be modeled. Thyroid nodule detection in such images imposes the use of a segmentation method that takes into consideration their inherent noise characteristics. Active contour models have not been employed for the accurate detection of thyroid nodules in ultrasound images [18].

Chunming Li et al. 2005 proposed a new level set formulation that completely eliminates the need of the re-initialization. The proposed level set method can be easily implemented by using simple finite difference scheme. It is computationally more efficient than the traditional level set methods. The level set function is no longer required to be initialized

as a signed distance function. This model is a region-based initialization of level set function, which is not only computationally more efficient than computing signed distance function, but also allows for more flexible applications [19].

Umasankar Kandaswamy et al. 2005 considered the problem of computation in Synthetic Aperture Radar (SAR) texture analysis and proposed a method for efficient analysis of image texture based on the notion of approximate features. That is, rather than using the entire image data for the analysis, they used an approximation of the image. For SAR imagery, texture analysis usually requires a consideration of both the micro- and macro-textural structures in the image. Some SAR image analysis problems involve high-rate, high-quality multi-channel and multi-temporal images, with image sizes running into millions of pixels. [20]

Arati S. Kurani et.al 2006 proposed a new approach to the co-occurrence matrix currently used to extract textural features: *co-occurrence matrices for volumetric data.* In traditional texture metrics have concentrated on 2D texture, 3D imaging modalities are becoming more and more prevalent. In this paper textural features derived from 2D are compared to those results derived from using co-occurrence matrices for volumetric data. indicate that the volumetric texture features have better discriminating power than 2D texture derived from slice data.[21]

CHAPTER 3

TECHNIQUES USED

In introduction this thesis explains different techniques available for segmentation and texture analysis. This section explains about the method used in this thesis. Level-set method of segmentation of medical images and Statistical method of texture analysis method for extracting the texture features from the images are used. These are explained one by one.

3.1 Digital image

An analog image converted to numerical form so that it can be stored and used in a computer. It is composed of discrete pixels of digitally quantized brightness and color. The image is divided into a matrix of small regions called picture elements or pixels. At sub-satellite point each pixel represents a specific amount of area. For example, in APT each pixel represents 4.1 kilometers. Each pixel has a numerical value or data number value, quantifying the radiance of the image at that spot. The data number value of each pixel usually represents a value between black and white, i.e., shades of gray.

3.2 Types of digital image

JPG, GIF, TIFF, PNG, BMP etc are the types of digital images. These are explained below:

TIFF (**Tagged Image File Format**) is a very flexible format that can be lossless or lousy. The details of the image storage algorithm are included as part of the file. In practice, TIFF is used almost exclusively as a lossless image storage format that uses no compression at all.[23] Most graphics programs that use TIFF do not compression. Consequently, file sizes are quite big. (Sometimes a lossless compression algorithm called LZW is used, but it is not universally supported.)

PNG (**Portable Network Graphics**) is also a lossless storage format. However, in contrast with common TIFF usage, it looks for patterns in the image that it can use to compress file size. The compression is exactly reversible, so the image is recovered exactly.

GIF (**Graphics Interchange Format**) creates a table of up to 256 colors from a pool of 16 million. If the image has fewer than 256 colors, GIF can render the image exactly. When the image contains many colors, software that creates the GIF uses any of several algorithms to approximate the colors in the image with the limited palette of 256 colors available. Better algorithms search the image to find an optimum set of 256 colors. Sometimes GIF uses the nearest color to represent each pixel, and sometimes it uses "error diffusion" to adjust the color of nearby pixels to correct for the error in each pixel.

JPG (**Joint Photographic Experts Group**) is optimized for photographs and similar continuous tone images that contain many, many colors. It can achieve astounding compression ratios even while maintaining very high image quality. GIF compression is unkind to such images. JPG works by analyzing images and discarding kinds of information that the eye is least likely to notice. It stores information as 24 bit color. The degree of compression of JPG is adjustable. At moderate compression levels of photographic images, it is very difficult for the eye to discern any difference from the original, even at extreme magnification. Compression factors of more than 20 are often quite acceptable.

RAW is an image output option available on some digital cameras. Though lossless, it is a factor of three of four smaller than TIFF files of the same image. The disadvantage is that there is a different RAW format for each manufacturer, and so you may have to use the manufacturer's software to view the images.

BMP File Format sometimes called **bitmap** or **DIB file format** (for device-independent bitmap), is an uncompressed proprietary format invented by Microsoft. There is really no reason to ever use this format.

PSD, PSP, etc. are proprietary formats used by graphics programs. Photoshop's files have the PSD extension, while Paint Shop Pro files use PSP. These are the preferred working formats as you edit images in the software, because only the proprietary formats retain all the editing power of the programs.

Currently, GIF and JPG are the formats used for nearly all web images. PNG is supported by most of the latest generation browsers. TIFF is not widely supported by web browsers, and should be avoided for web use. PNG does everything GIF does, and better, so expect

to see PNG replace GIF in the future. PNG will not replace JPG, since JPG is capable of much greater compression of photographic images, even when set for quite minimal loss of quality

3.3 Medical imaging

Medical imaging refers to the techniques and processes used to create images of the human body for clinical purposes. In the clinical context, medical imaging is generally equated to radiology or "clinical imaging" and the medical practitioner responsible for interpreting the images is a radiologist. Diagnostic radiography designates the technical aspects of medical imaging and in particular the acquisition of medical images. The radiographer or radio-logic technologist is usually responsible for acquiring medical images of diagnostic quality. As a field of scientific investigation, medical imaging constitutes a sub-discipline of biomedical engineering, medical physics or medicine depending on the context: Research and development in the area of instrumentation, image acquisition (e.g. radiography), modeling and quantification are usually the preserve of biomedical engineering, medical physics and computer science; Research into the application and interpretation of medical images is usually the preserve of radiology and the medical sub-discipline relevant to medical condition or area of medical science (neuroscience, cardiology, psychiatry, psychology, etc) under investigation. Many of the techniques developed for medical imaging also have scientific and industrial applications.

3.4 Types of medical imaging

3.4.1 Computed tomography (CT)

Computed tomography (CT) scans are often called "**cat scans**." CT scans use the same technology as an X-ray but in a three dimensional way. Instead of the flat pictures in a standard X-ray, a CT scan offers several images, sometimes called slices. This offers medical professionals the chance to view not just a frontal view of an organ but an inner, outer, and view within. CT image is shown in fig 1.1. [24]

Fig 3.1: Commutated tomography

3.4.2 Magnetic Resonance Imaging (MRI)

MRI uses a magnet to line hydrogen atoms in the human body to allow them to receive radio waves. The body sends back a radio signal back to the MRI machine which is converted into detailed images of the body part.

CT and MRI being sensitive to different properties of the tissues. In CT, X-rays must be blocked by some form of dense tissue to create an image, therefore the image quality when looking at soft tissues will be poor but it is not their in MRI

3.4.3 Ultrasounds

Ultrasounds are a form of sonography. Pregnant women usually receive at least one ultrasound to determine if the fetus is developing properly. Some medical issues can be determined through ultrasound and repaired before birth with fetal surgery. Ultrasounds are also often used to detect gallstones or tumors. It's called an ultrasound because high frequency sound waves are sent into the body and the echo that comes back provides an image.

It provide less anatomical information than techniques such as CT or MRI, but it studies the function of moving structures in real-time. It is also very safe to use, as the patient is not exposed to radiation and the ultrasound does not appear to cause any adverse effects.

3.5 CT Scan

CT was discovered independently by a British engineer named Sir Godfrey Hounsfield and Dr. Alan Cormack. It has become a mandatory method for diagnosing medical diseases. CT scanners first began to be installed in 1974. Because of advances in computer technology, CT scanners

have vastly improved patient comfort because they are now much faster. These improvements have also led to higher-resolution images, which improve the diagnostic capabilities of the test. For example, the CT scan can show doctors small nodules or tumors, which they cannot see on an X-ray.

Procedure

CT or CAT scans are special x-ray tests that produce cross-sectional images of the body using x-rays and a computer. These images allow the radiologist, a medical doctor who specializes in images of the body, to look at the inside of the body just as you would look at the inside of a loaf of bread by slicing it. This type of special x-ray, in a sense, takes pictures of slices of the body so doctors can look right at the area of interest. CT scans are frequently used to evaluate the brain, neck, spine, chest, abdomen, pelvis, and sinuses.

The pictures produced by CT scans are called tomograms. The CT scanner is a large machine shown in fig 3.2. The pictures are taken while patient lie on a couch, which moves backwards and forwards through the hole of the machine that is shaped rather like a giant doughnut. For CT scan, patient will be required to lie on a motorized couch inside the scanning machine which looks like a giant doughnut. The scan may need a contrast dye or substance that improves the picture of certain tissues or blood vessels. This material may be swallowed, given as an enema or injected into the blood stream, depending on the part of the body that is to be scanned. A CT scanner uses a series of X-ray beams to build up images of the body in slices. Unlike an X-ray, which sends one beam of radiation through the body, a CT scanner emits a succession of narrow beams as it moves through an arc. This produces a very detailed image that is not possible from a normal X-ray. The X-ray detector within a CT scanner can see hundreds of different levels of density, including tissues within solid organs such as the liver. This information is then sent to a computer, which builds up a cross-sectional image of the body and displays it on the screen. Depending on the part of the body being examined, a contrast dye may be used to make some tissues show up more clearly under X-ray. For scans of the abdomen, you might be given a drink containing barium. This is known as a barium meal, and shows up white on the scans as it moves through the digestive tract. The X-ray beam takes a continuous spiral path during scanning, gathering continuous data with no gaps between images. CT scans are commonly performed on the head and abdomen.

Head scans are an effective method of checking the brain for suspected tumors, bleeding, or swelling of the arteries. They are also useful for investigating the brain following a stroke.

Abdominal CT scans are used to detect tumors and to diagnose conditions in which internal organs, including the liver, kidneys, pancreas, intestines, and lungs are enlarged or inflamed. CT scanning can identify normal and abnormal tissue, making it a useful tool to plan areas for radiotherapy treatments and as a guide for taking tissue samples and needle biopsies.

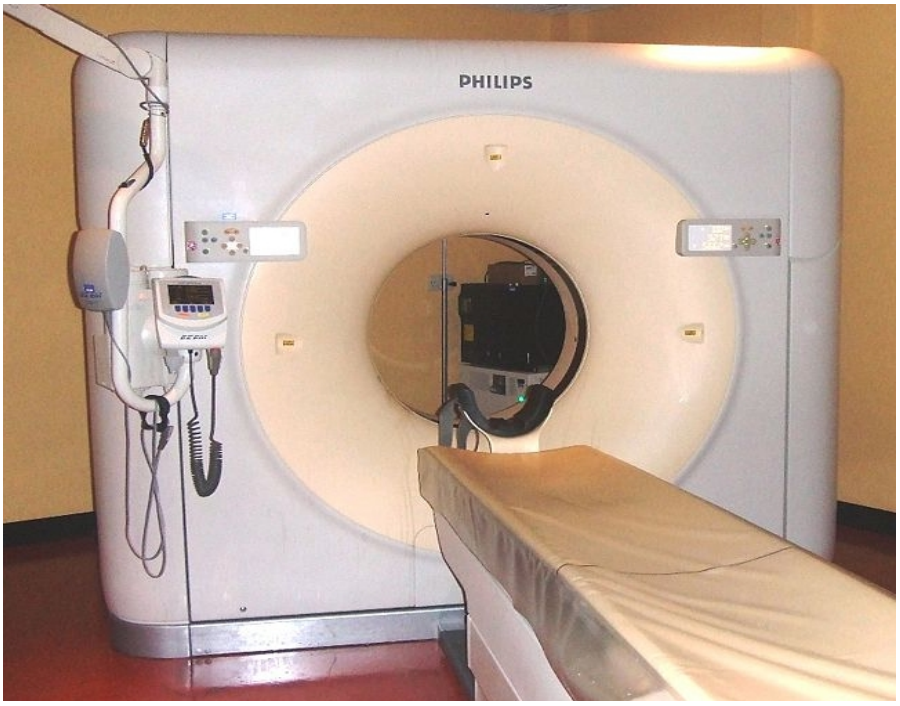

Fig.3.2: CT scan machine

Risks

CT scans involve exposure to radiation in the form of X-rays. The level of radiation used is kept to a minimum to prevent damage to body cells and the dose is said to be about the same as the average person receives from background radiation in three years. CT scans are quick and accurate, and they eliminate the need for invasive surgery. The benefits of having a scan outweigh any risks and it is generally considered very safe.

Pregnant women should not have a CT scan, as there is a small risk that X-rays may cause an abnormality to the unborn child. Be sure to tell your doctor if you think there is a chance that you may be pregnant before having a scan.

The contrast dye used in CT scans often contains iodine, which can cause an allergic reaction in a few people. You should inform the radiologist if you have had an allergic reaction to iodine or a contrast dye in the past, or if you have any other allergies. Very rarely the dye may cause some kidney damage in people who already have kidney problems.

Nursing mothers should wait for 24 hours after a scan using a contrast dye before resuming breastfeeding.

3.5 Anatomy of abdomen

These are axial views of the upper abdomen shown by Computed Tomography image [25]. The brief description of the various parts of the abdomen is explained below:

(1) **Liver** is made up of four different lobes: the right lobe, left lobe, caudate lobe, and quadrate. The right lobe of the liver occupies the right upper quadrant. The left lobe is much smaller and has a different blood supply and portal drainage from the right lobe. It is covered by a thin capsule of Glisson which causes pain when it is stretched by an enlarging liver. The caudate lobe is functionally part of both right and left lobes because it receives its blood supply from both right and left hepatic arteries. The quadrate lobe receives its blood supply form the left hepatic artery and is therefore functionally part of the left lobe. .

(2) **Spleen** is located in the left upper quadrant. Its upper pole is related to the lower ribs. The most inferior part of the spleen extends to L2. The tip of the spleen is usually palpable only when it is enlarged in pathologic conditions such as leukemia.

(3) **Pancreas** is located in epigastrum. It is divided into four parts: head (3+ on images), body, tail (3*), and uncinate process (3-).

(4) **Gallbladder** is an organ that sits in between the right and quadrate lobes of the liver.The function of the gallbladder are to store bile produced by the liver. It contracts to release bile when the enzyme cholecystekinin is secreted by the cells of the duodenum.

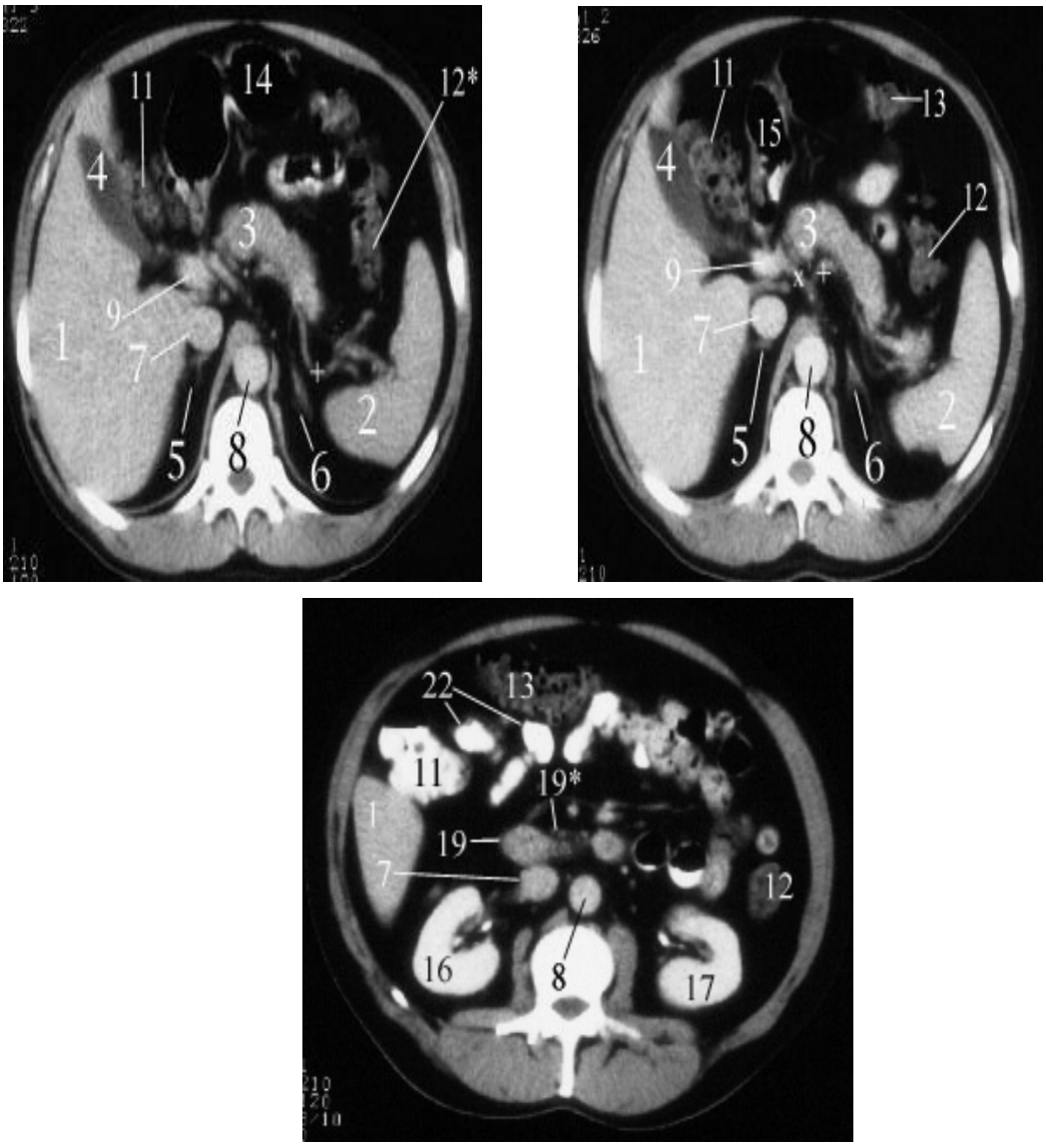

Fig 3.2: Various parts of abdomen

(5) **Right Adrenal Gland** lies superior and medial to the kidney. The right adrenal gland is said to be horseshoe-shaped. The adrenal gland is divided into the medulla and the cortex.

(6) **Left Adrenal Gland** is located higher than the right adrenal gland.

(7) **Inferior Vena Cava** is a large vein that returns blood from the blood in the lower part of the body. It is a reservoir for the common iliac, lumbar, right gonadal, renal, right adrenal, and hepatic veins

(8) **Aorta** travels in the abdomen anterior to the vertebrae. The aorta maintains a relation to the left of the inferior vena cava.

(9) **Portal Vein** is formed by the confluence of the inferior mesenteric, superior mesenteric, and splenic veins. The portal veins brings nutrients absorbed from the intestines into the liver where the cells process the nutrients.

(10) **Superior Mesenteric Artery** is the second branch of the abdominal aorta (the first is the celiac trunk).

(10*) **Superior Mesenteric Vein** drains the blood coming from the small intestine and empties it into the portal vein..

(11) **Ascending Colon** is the first part of the colon and it lies on the right side of the abdomen.

(12) **Descending Colon** is retroperitoneal and derives its blood supply from the left colic branch of the inferior mesenteric artery..

(13) **Transverse Colon** is intraperitoneal because it is suspended by the part of the mesentery called the transverse mesocolon. It begins at the hepatic flexure and ends at the splenic flexure.

(14) **Stomach** is made up of the cardia, fundus, body, antrum and pylorus .

(15) **Distal Stomach** consists of the pylorus, antrum, and part of the body. The antrum forms the beginning of the distal stomach

(16) **Right Kidney** is a retroperitoneal organ that is located in the posterior abdomen. The right kidney is situated 2-8 cm lower than its left counterpart because of the large liver which sits superior to it. The structure of the kidney is complex. The function of the kidney is to regulate the electrolyte and water balance in the body.

(17) **Left Kidney** is higher than the right kidney.

(18) **Inferior Mesenteric Artery** (Not visualized) provides blood supply to the embryological hindgut organs including the distal transverse colon, descending colon and sigmoid colon.

(19) **Duodenum** is the first part of the small intestine. It is also the shortest part

(20) **Left Renal Vein** courses between the aorta and superior mesenteric artery to join the inferior vena cava..

(20*) **Left Renal Artery** originates from the abdominal aorta at about L1 or L2, below the origin of the superior mesenteric artery.

(21) **Right Renal Vein** is anterior to the right renal artery. It is shorter than the left vein.

(21*) **Right Renal Artery** originates from the aorta at about L1 or L2.

(22) **Small Intestine** is the longest part of the gastrointestinal tract, usually measuring 6-7meters.

3.6 Level-set method of segmentation

In recent years, a large body of work on geometric level-sets, i.e., level-sets implemented via level set methods, has been proposed to address a wide range of image segmentation problems in image processing and computer vision. Segmenting images with level set methods was introduced at the end of the 1980's by Sethian and Osher [22] in the context of modeling propagating fronts described by a number of physical phenomenons and was based on previous work on moving curvatures. Since then several variants and improvements have come up. Some of the improvements are aimed at speeding up the processing. Other methods have strength related to specific challenges like noise and broken edges.

In the level set method, the curve is represented implicitly as a level set of a 2D scalar function referred to as the level set function, which is usually defined on the same domain as the image. The level set is defined as the set of points that have the same function value. The advantage of the level set method is that one can perform numerical computations involving curves and surfaces on a fixed Cartesian grid without having to parameterize these objects (this is called the Eulerian approach). Also, the level set method makes it very easy to follow shapes that change topology, for example when a shape splits in two, develops holes, or the reverse of these operations. The existing level-set models can be broadly classified as either parametric level-set models or geometric level-set models according to their representation and implementation. In particular, the parametric level-sets are represented explicitly as parameterized curves in a Lagrangian framework, while the geometric level-sets are represented implicitly as level sets of a two-dimensional function that evolves in an Eulerian framework. Geometric level-sets models are based on curve evolution theory and level set method. The basic idea is to represent level-sets as the zero level set of an implicit function defined in a higher dimension, usually referred as the level set function, and to evolve the level set function according to a partial differential equation (PDE). This approach presents several advantages over the traditional parametric level-sets.

First, the level-sets represented by the level set function may break or merge naturally during the evolution, and the topological changes are thus automatically handled. Second, the level set function always remains a function on a fixed grid, which allows efficient numerical schemes. Early geometric level-set models are typically derived using a Lagrangian formulation which uses a certain evolution PDE of a parametrized curve. Compared with pure PDE driven level set methods, the variational level set methods are more convenient. Chan and Vese [9] proposed a level-set model using a variational level set formulation. By incorporating region-based

information into their energy functional as an additional constraint, their model has much larger convergence range and flexible initialization. In implementing the traditional level set methods, it is numerically necessary to keep the evolving level set function close to a signed distance function. Re-initialization, a technique for periodically re-initializing the level set function to a signed distance function during the evolution, has been extensively used for maintaining stable curve evolution and ensuring usable results. In this thesis we used level-set without re-initialization proposed by chunming Li et.al [19].

3.6.1 Traditional level set method

In level set formulation of level-sets, the level-set is denoted by C, are represented by the zero level set

$$C(t) = \{(x, y) \mid \phi(t, x, y) = 0\} \quad \text{.....3.1}$$

of a level set function ϕ (t, x, y). The evolution equation of the level set function ϕ can be written in the following form:

$$\frac{\partial \phi}{\partial t} + F|\nabla \phi| = 0 \quad \text{.....3.2}$$

which is called level set equation. The function F is called the speed function. For image segmentation, the function F depends on the image data and the level set function ϕ . In this method of level set problems are the level set function can develop shocks, very sharp and flat shape during the evolution, To avoid these problems, a common numerical scheme is used that is to initialize the function ϕ as a signed distance function before the evolution, and then reshape the function ϕ to be a signed distance function periodically during the evolution.

The re-initialization method is to solve the following re-initialization Equation

$$\frac{\partial \phi}{\partial t} = sign(\phi_0)(1 - |\nabla \phi|) \quad \text{.....3.3}$$

where ϕ_0 is the function to be re-initialized, and sign(ϕ) is the sign function. But problem is there if ϕ_0 is not smooth or ϕ_0 is much steeper on one side of the interface than the other, the

zero level set of the resulting function ϕ can be moved incorrectly from that of the original function. For removing this limitation we use new approach of Variational Level Set Formulation of Curve Evolution without Re-initialization by Chunming Li et.al [19].

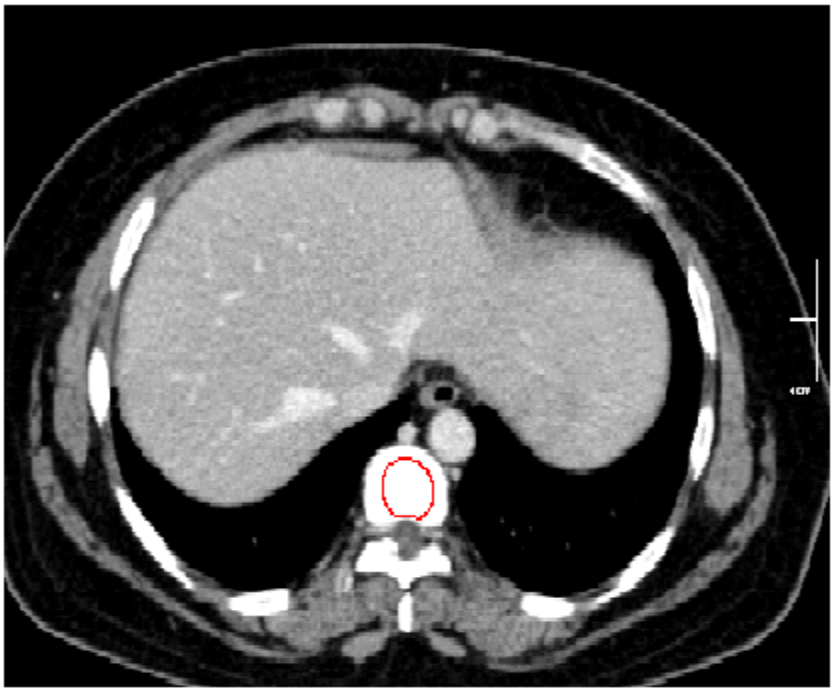

Fig 3.3: Level-set after 20 iteration

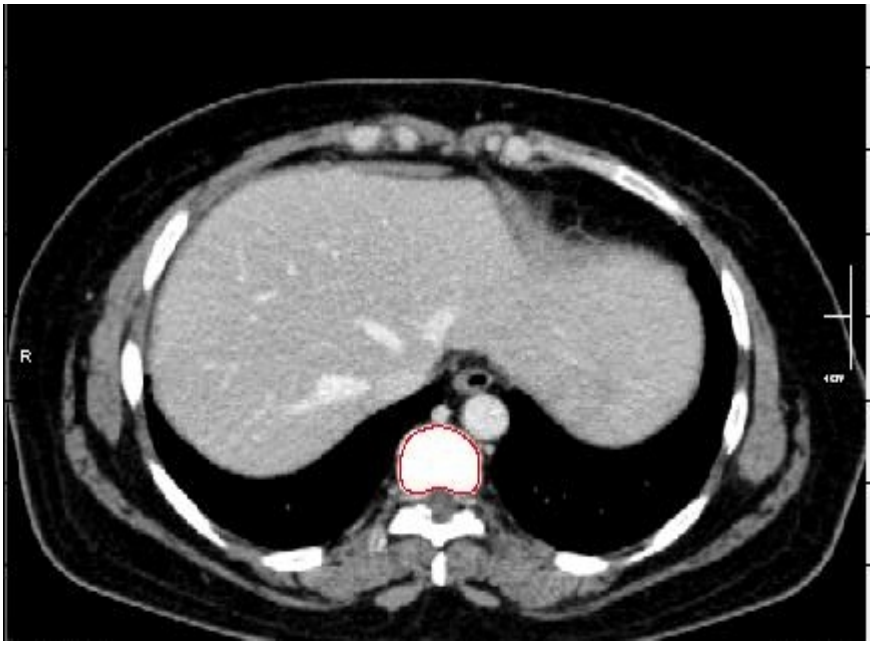

Fig 3.4: Level set after 300 iteration (Final level-set)

3.6.1 Variational level set formulation of curve evolution without re-initialization

We know that level-set are dynamic curves that move toward the object boundaries. Therefore we define an external energy that can move towards the edges. If I be the image, then edge indicator function (g) is defined by:

$$g = \frac{1}{1+\left|\nabla G_\sigma * I\right|^2} \quad \ldots\ldots\ldots\ldots\ldots\ldots\ldots\ldots\ldots\ldots\ldots\ldots 3.4$$

where G_σ is the Gaussian kernel with standard deviation σ. We define an external energy for a function ϕ (x, y) as below:

$$E_{g,}\,\lambda,\ \alpha\,(\phi) = \lambda L_g\,(\phi) + \alpha\, A_g\,(\phi) \ldots\ldots\ldots\ldots\ldots\ldots\ldots 3.5$$

where $\lambda > 0$ and α are constants, and the terms $L_g(\phi)$ and $A_g(\phi)$ are defined by

$$L_g(\phi) = \int_\Omega g\varepsilon(\phi)|\nabla\phi|dxdy \quad \text{.....3.6}$$

and,

$$A_g(\phi) = \int gH(-\phi)dxdy \quad \text{.....37}$$

respectively, where ε is the univariate Dirac function, and H is the Heaviside function. Now, the following total energy functional

$$E(\phi) = \mu P(\phi) + Eg, \lambda, \alpha\ (\phi) \quad \text{.....3.8}$$

The external energy E_g, λ, α drives the zero level set toward the object boundaries, while the internal energy $\mu P(\phi)$ penalizes the deviation of ϕ from a signed distance function during its evolution which is give in equation given below.

$$p(\phi) = \int_\Omega \frac{1}{2}(|\nabla\phi| - 1)^2 dxdy \quad \text{.....3.9}$$

The variational formula derive from the penalize energy equation

$$E(\phi) = \mu.p(\phi) + E_m \quad \text{.....3.10}$$

where $\mu > 0$ is a parameter controlling the effect of penalizing the deviation of ϕ from a signed distance function, and $E_m(\phi)$ is a certain energy that would drive the motion of the zero level curve of ϕ.

The energy functional Ag (ϕ) introduced to speed up curve evolution. The coefficient α of A_g can be positive or negative, depending on the relative position of the initial level-set to the object of interest. For example, if the initial level-sets are placed outside the object, the coefficient α in the weighted area term should take positive value, so that the level-sets can shrink faster. If the initial level-sets are placed inside the object, the coefficient

α should take negative value to speed up the expansion of the level-sets. By calculus of variations, the Gateaux derivative of the functional *E* in can be written as

$$\frac{\partial E}{\partial \phi} = -\mu[\Delta\phi - div(\frac{\nabla\phi}{|\nabla\phi|})] - \lambda\delta(\phi)div(g\frac{\nabla\phi}{|\nabla\phi|}) - \alpha g\varepsilon(\phi) \text{ .....3.9}$$

where Δ is the Laplacian operator, Therefore, the function ϕ hat minimizes this functional satisfies the Euler-Lagrange equation $\frac{\partial E}{\partial \phi} = 0$ .the gradient flows of the energy function $\lambda Lg(\phi)$ and $\alpha Ag(\phi)$,are responsible of driving the zero level curve towards the object boundaries.

So this new approach of level-sets is tested on medical images like ultrasound, CT and MRI. It shows good result on medical images even on more noisy images. But one problem is there that is we have to make the level-set optimized to the particular image, and if images changes than topology has to change by user itself.

3.7 Problems in level-set method

In level-set method, results are coming fine and the topology is easily changed by changing its parameters of equations describe above. But for finding optimized we have to change the parameters according to the image. Different image have different character and it segmented by different parameters shown in figure below:

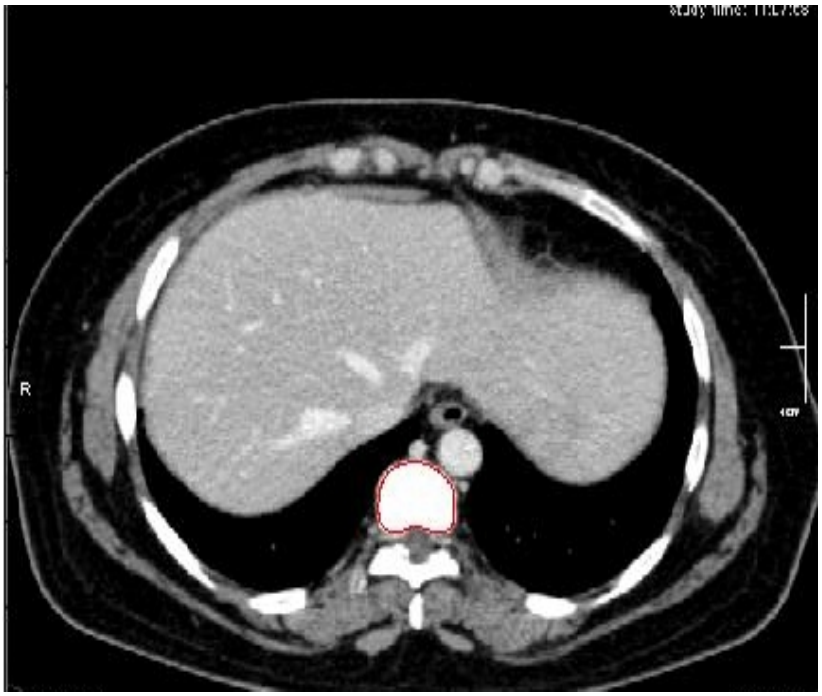

Fig3.5: Optimized segmentation at different parameters- alpha=-1.5, lambda=6,timestep=7,iteration=100, epsilon=3.

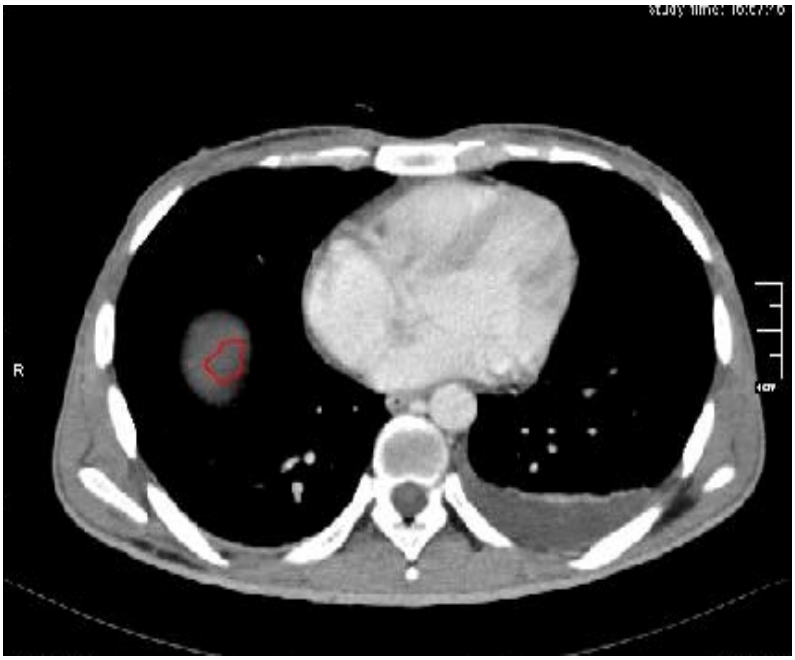

Fig 3.6: Inaccurate Segmentation (it using pervious values of level-set parameters which show that they are not optimal for this image).

Fig3.7: Optimized segmentation –alpha=3,lambda=6,timestep=7,iteration=100, epsilon=3.

So to get those particular parameters of level-set for segmentation we have to identify the image feature. For this we used texture analysis. In texture analysis I calculated the texture features given in table 3.1. Now these features show the characteristics of an image and indirectly depend upon the level-set parameters. Now main problem is that how we will select the level-set parameters according to texture features. The answer is fuzzy logic, fuzzy logic give us the values of level-set parameters by defining user define rules from the texture features for example:

if the entropy is low and energy is low then

alpha is low and lambda is low.

This implementation is described in next section Methodology.

3.8 Statistical method of texture analysis

Another approach I used in my thesis is Statistical methods of texture analysis. One of the defining qualities of texture is the spatial distribution of gray values. In the following {I(x, y), 0< x >N– 1, 0< y >N– 1}[23] is used to denote an image with gray levels. A

large number of texture features have been proposed. But, these features are not independent. The relationship between the various statistical texture measures and the input image is summarized in Figure 3.3. [23]

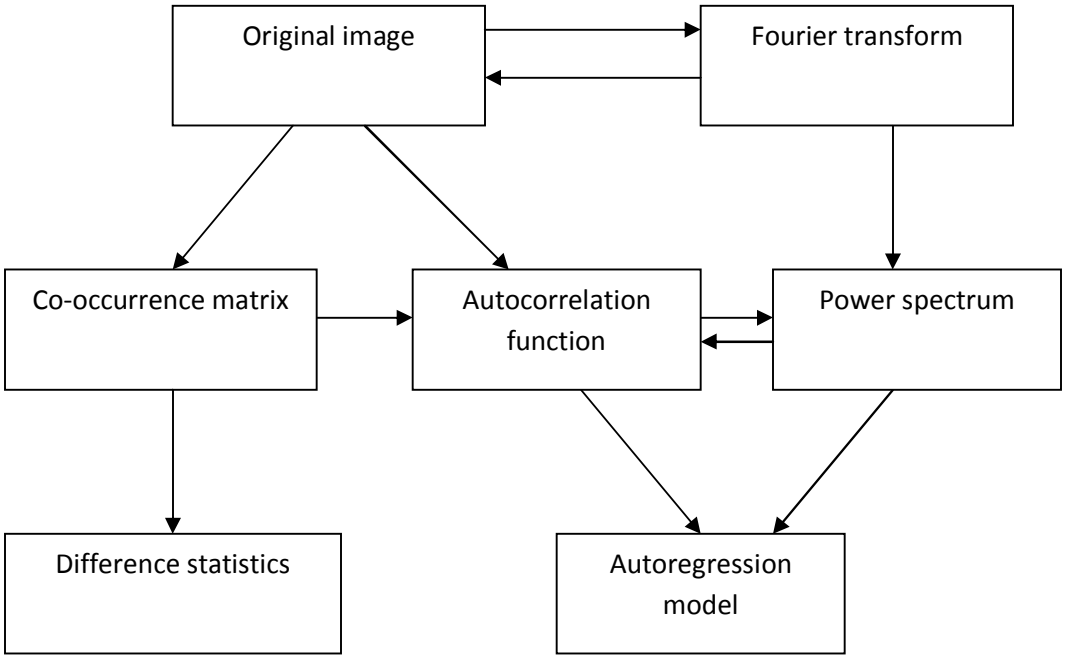

Fig 3.3: The interrelation between the various second-order statistics and the input image

Co-occurrence matrices

Spatial gray level co-occurrence estimates image properties related to second-order statistics. Gray level co-occurrence matrices (GLCM) widely used texture features. The G*G gray level co-occurrence matrix P_d for a displacement vector d =(dx, dy) is defined as follows. The entry (i, j) of P_d is the number of occurrences of the pair of gray levels i and j which are a distance apart. Formally, it is given as

$$P_d(i, j) = \left|\{((r, s), (t, v)) : I(r, s) = i, I(t, v) = j\}\right| \quad \text{.....3.10}$$

where (r, s),(t, v) ε N*N, (t, v) = (r + dx, s + dy) and $|.|$ is the cardinality of a set I used this analysis for getting the information in the medical images and store these in numerical form. So that I can use it for optimization of medical images. I calculated various textural features from gray co-occurrence method, including Entropy, Energy, Contrast, Homogeneity, Mean, standard Variance, Correlation. The formulae for all these texture features are describe in table 3.1.

Table3.1: Explanation of different texture features

Feature	**Formula**	**What is measured?**
Entropy	$-\sum_{i}^{m}\sum_{j}^{n} P[i,j]\log P[i,j]$	Measures the randomness of a gray-level distribution. The Entropy is expected to be high if the gray levels are distributed randomly through out the image.
Energy	$\sum_{i}^{m}\sum_{j}^{n} P^2[i,j]$	Measures the number of repeated pairs. The Energy is expected to be high if the occurrence of repeated pixel pairs is high

Contrast	$\sum_{i}^{m} \sum_{j}^{n} (i-j)^2 P[i,j]$	Measures the local contrast of an image. The Contrast is expected to be low if the gray levels of each pixel pair are similar.
Homogeneity	$\sum_{i}^{m} \sum_{j}^{n} \frac{P[i,j]}{1+\lvert i-j \rvert}$	Measures the local homogeneity of a pixel pair. The Homogeneity is expected to be large if the gray levels of each pixel pair are similar
Mean	$\frac{1}{2}\sum_{i}^{m} \sum_{j}^{n} (iP[i,j] + jP[i,j])$	Provides the mean of the gray levels in the image. The Mean is expected to be large if the sum of the gray levels of the image is high
Standard Variance	$\frac{1}{2}\sum_{i}^{m} \sum_{j}^{n} (i-\mu)^2 P[i,j] + (j-\mu)^2 jP[i,j]$	Variance tells us how spread out the distribution of gray levels is. The Variance is expected to be large if the gray levels of the image are spread out greatly

Correlation	$\sum_{i}^{m} \sum_{j}^{n} \frac{(i-\mu)\ (j-\mu)P[i,j]}{\sigma^2}$	Provides a correlation between the two pixels in the pixel pair. The Correlation is expected to be high if the gray levels of the pixel pairs are highly correlated.

The co-occurrence matrix features suffer from a number of difficulties. There is no well established method of selecting the displacement vector d and computing co-occurrence matrices for different values d of is not feasible. For a given d, a large number of features can be computed from the co-occurrence matrix. This means that some sort of feature selection method must be used to select the most relevant features. The co-occurrence matrix-based texture features have also been primarily used in texture classification tasks and not in segmentation tasks.

CHAPTER 4

METHODOLOGY

First of all we would like to thanks Chunming Li for his MATLAB code for level-set with out re-initialization. This thesis work is to modify the existing code to get better results. The description and modification that has done is described in this chapter.

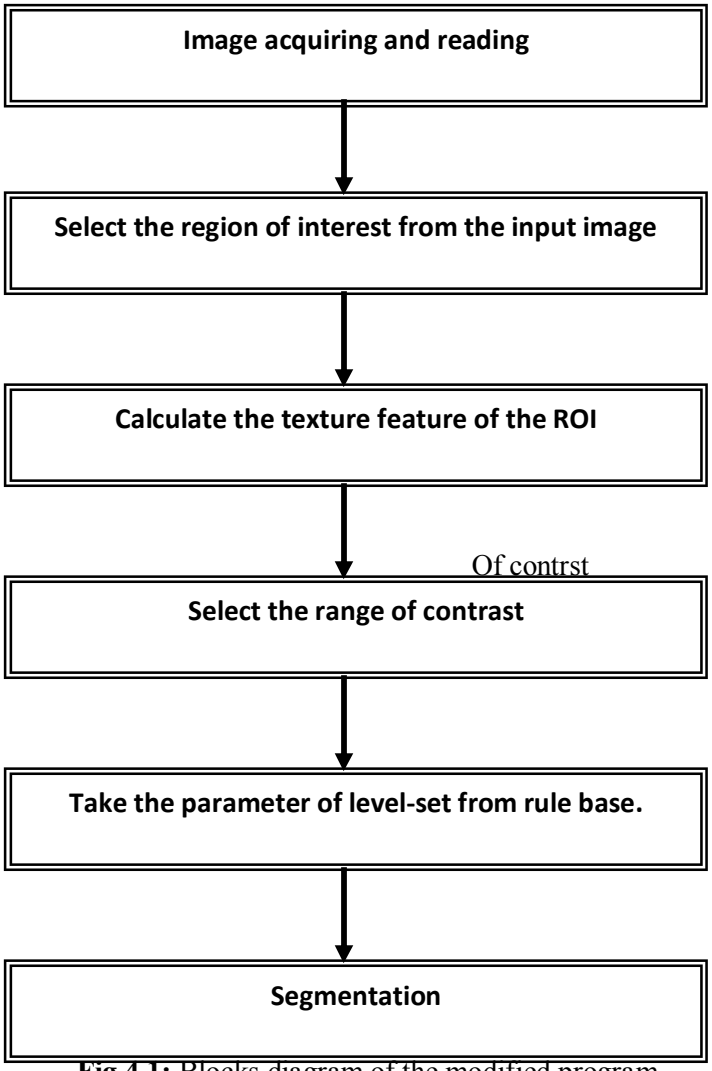

Fig 4.1: Blocks diagram of the modified program

4.1 Algorithm

Step 1:- Firstly the image was read with help of imread command. This command is inbuilt command in matlab processing toolbox. While reading the image we has to take care of one thing is that the image should not be of compressed .tiff file format because it could not be acceptable in matlab.

Step 2:- Now the matrix values are converted into more uniform and simplify form so that further calculation can become easy with help of mathematical formula

f = I x. ^2+Iy. ^2……....4.1

Step 3:- After this image is filtered with the help of Gaussian filter. The Gaussian filter is the basic filter. Generally Gaussian filter is use to remove the noise from the image so as to make image more sharp and smooth. The Gaussian filter smoothness or blurs an image by performing a convolution operation with a Gaussian filter kernel.

Step 4:- Now preprocessed image is further processed and calculated its gradient. Now this gradient image is used to calculate the edges of the image. For calculation of edges one function is used that is

$$g = \frac{1.}{1+f} \text{ .....4.2}$$

Step 5:- In this step all Parameters are defined which change the topology of the level-set means speed, stability etc. The parameters are alpha, time step, MU, lambda, epsilon refer section 3.6.

Step 6:- Initialization of level-set, means starting shape of level-set which is depend upon the region. Mainly it has to start from the centre of tumor in medical image because in medical images their many other body parts of body make many edges so if it start from outside the image or tumor then it stop on other edges not on the tumor edges. So in this it start from center by

making a polygon by mouse click inside the tumor using this command. It creates a polygon and this value has to give to level-set function

Step 7:-. In this step we gave all parameters and the initial level-set to the evolution function. This evolution function updates the level set function according to the level set evolution. The simple idea of the curve evolution is to reduce the set of vertices of the polygon to a subset of vertices containing important information about the original level-set.

Step 8:- The step 7 repeat until we will not get final level-set. The repetition is depending on the number of iteration given.

Step 9:- In last step, final level-set will display after all iterations. The updated value from evolution function is given to the function level-set and at end of the iterations it gives us final level-set.

4.2 Changes made in algorithm

For making the code automatic optimized we has to give the exact values of level-set parameters. So change made in step 5 all other code is same. The changes are described below:

Step 1:- First of all extract the interested part from the whole image, means the structure in the medical image. This is because it is the part which have the differ values than the other part of image and from the tumor of other image. The tumor part is abnormalities in the image so it has different characteristics. For extraction of tumor region we used ROI (region of interest) program. It is describes below

In ROI program we extract the region of interest from the image. In this, first give the image and after that number of region you want. It can be for multiple region also, but in one image mainly only one tumor is their so generally take it one only. It is given as

Roi = roi (I, nroi)

Where ‘I’ is the image and nroi is the number of ROI.

In this program getline ('closed') is used to get the polygon interactively, please click left mouse button to select, and right button to finish up a ROI (Backspace to delete the latest click). You may repeat this process till all ROIs were processed.

[X, Y] = GETLINE (I, ‘closed ')

returns a closed polygon. Coordinates of the polygon are returned in X and Y.

After this we used INPOLYGON. It is for getting points inside or on a polygonal region.

IN = INPOLYGON(X, Y, XV, YV)

returns a matrix IN the size of X and Y. By this we got another image for processing.

Step 2:- Next step is to calculate the texture features from the region which we extract from the ROI program.

```
roi.mean (1)          =   mean2 (roicidata (k_inside));
roi.std (1)           =   std2 (roicidata (k_inside));
roi.min (1)           =   min (roicidata (k_inside));
roi.max (1)           =   max (roicidata (k_inside));
roi.median (1)        =   median (roicidata (k_inside));
roi.entropy (1)       =  entropy (roicidata (k_inside));
roi.contrast (1)      =  graycoprops (roicidata (k_inside),'contrast')
roi.correlation (1)   =  graycoprops (roicidata (k_inside),'correlation')
roi.energy (1)        =  graycoprops (roicidata (k_inside),'energy')
roi.homogeneity (1)   =  graycoprops (roicidata (k_inside),'homogeneity')
```

where K_inside is the image extracted from the main image and all other are the function in matlab like mean2, std2, min, max, median, entropy. And others like contrast, correlation, energy and homogeneity are calculated by a special function called graycoprops.

STATS = GRAYCOPROPS (GLCM, PROPERTIES)

It is inbuilt function of matlab. It normalizes the gray-level co-occurrence matrix (GLCM) so that the sum of its elements is one [26]. It uses the normalized GLCM to calculate properties according to the formula given in table 3.1

GLCM can be an m x n x p array of valid gray-level co-occurrence matrices. Each gray-level co-occurrence matrix is normalized so that its sum is one. PROPERTIES can be a comma-separated list of strings, a cell array containing strings, the string 'all', or a space separated string. They can be abbreviated, and case does not matter.

Properties:

'Contrast':-The intensity contrast between a pixel and its neighbor over the whole image. It value be zero for a constant image.

'Correlation':- Statistical measure of how correlated a pixel is to its neighbor over the whole image. Correlation is 1 or -1 for a perfectly positively or negatively correlated image.

'Energy':- Summation of squared elements in the GLCM. Energy is 1 for a constant image.

'Homogeneity':- Closeness of the distribution of elements in the GLCM to the GLCM diagonal. Homogeneity is 1 for a diagonal GLCM.

Step 3:- Now call the selection base program. This program chooses the appropriate values of level-set parameters form its database according to the if-else rules .The output of this control strategy are the input for the segmentation program. These parameters are the optimized parameter for the level set program.

If contrast (< 100), then

Alpha = 1.5 else

If (contrast >100 ‖ < 200), then

Alpha = 3, else

Alpha = 4

CHAPTER 5

RESULTS

In this work level-set method is automatically optimized using texture analysis and decision making rules for selection of optimized parameters of level-set based on the texture features. Here four main steps are taken

- Analysis of Textural features of the image.
- Getting the optimized level-set parameters
- Selection of best texture feature
- Run the segmentation code.

5.1 Analysis of textural features of the image.

In this work we used 5 different CT images for test my modified code of segmentation. The different features are calculated for these 5 images shown in table 5.1.all the features are calculating on the basis of statistical method of texture analysis [24].image is taken and select the region of image which has been segmented parts of images are like gallbladder, aorta etc explained in chapter 3.

Table 5.1: Texture features of different CT images

S.No.	Test images	Texture features
1		Evaluating area = 1744.50 Mean = 248.62 Std = 24.32 Contrast = 360.6527 Correlation = 0.0070 Energy = 5.6754e-004 Homogeneity = 0.1270
		Evaluating area = 586.00 Mean = 199.28 Std = 33.81 Contrast = 143.4023 Correlation = -0.1549 Energy = 0.0017 Homogeneity= 0.1706

2		Evaluating area = 706.50 Mean = 194.00 Std = 38.14 Contrast = 111.7609 Correlation = 0.2483 Energy = 0.0014 Homogeneity= 0.1844
		Evaluating area = 1685.50 Mean = 85.99 Std = 16.73 Contrast = 372.3147 Correlation= -0.0136 Energy= 5.9382e-004 Homogeneity= 0.1265

3		Evaluating area = 1629.00 Mean = 117.04 Std = 15.18 Contrast = 149.7252 Correlation = 0.6391 Energy = 6.1614e-004 Homogeneity = 0.1647
		Evaluating area = 498.00 Mean = 196.47 Std = 25.03 Contrast =130.8238 Correlation = -0.0541 Energy = 0.0019 Homogeneity= 0.1794

4	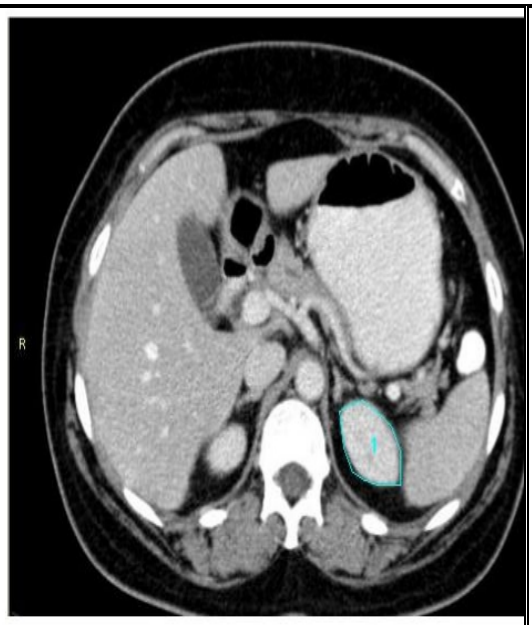	Evaluating area = 2122.00 Mean = 194.85 Std = 27.28 Contrast = 431.4984 Correlation = -0.0178 Energy = 4.7015e-004 Homogeneity = 0.0746
	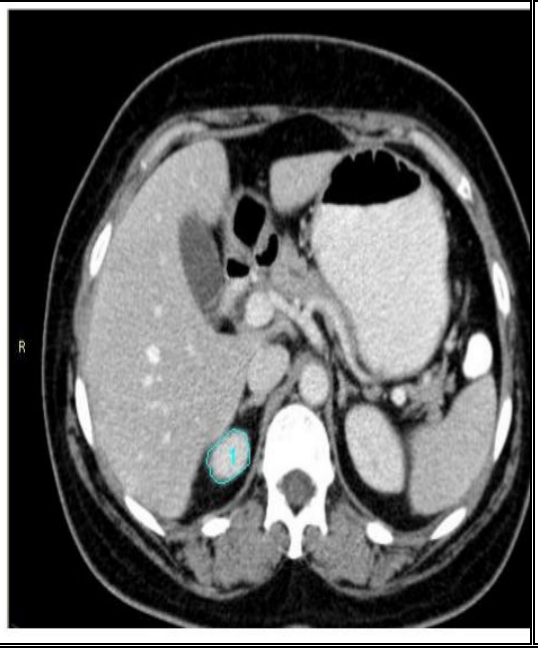	Evaluating area = 821.00 Mean = 184.29 Std = 35.54 Contrast = 194.4609 Correlation= 0.0030 Energy= 0.0012 Homogeneity= 0.1534

5	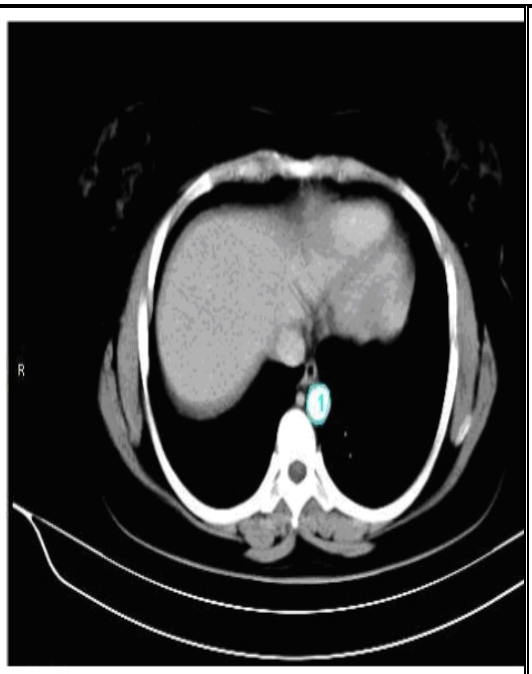	Evaluating area = 307.00 Mean = 246.02 Std = 22.60 Contrast = 89.4153 Correlation = -0.3460 Energy = 0.0032 Homogeneity = 0.1318
		Evaluating area = 146.00 Mean = 104.54 Std = 20.87 Contrast = 34.9530 Correlation= 0.0351 Energy = 0.0067 Homogeneity = 0.2662

5.3 Getting the optimized level-set parameters

Every image segmented with different level-set parameters, therefore in this steps optimized level-set parameter is calculated manually

Table 5.2: Segmentation the image with different parameters

S.No.	Tested parameters	Optimized parameters	Result of segmentation

1	Alpha=1.5,3,3.5 Lambda=5,6,7 Epsilon=1.5,3 Iterations=100,150, 200	Alpha=-3.5 Lambda=7 Epsilon=7 Iterations=200	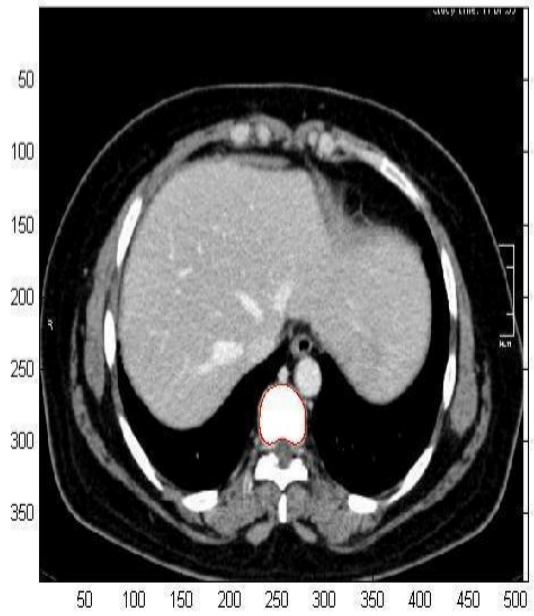
	Alpha=1.5,3,3.5 Lambda=5,6,7 Epsilon=1.5,3 Iterations=100,150, 200	Alpha=3 Lambda=7 Epsilon=7 Iterations=150	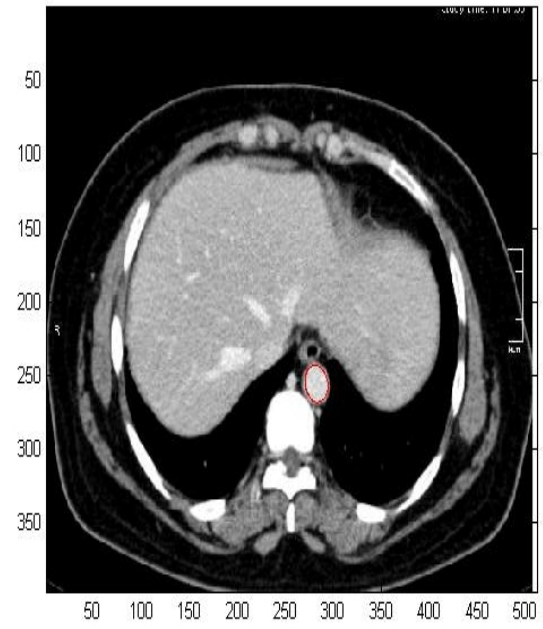

2	Alpha=1.5,3,3.5 Lambda=5,6,7 Epsilon=1.5,3 Iterations=100,150, 200	Alpha=-3 Lambda=7 Epsilon=7 Iterations=150	
	Alpha=1.5,3,3.5 Lambda=5,6,7 Epsilon=1.5,3 Iterations=100,150, 200	Alpha=-3.5 Lambda=7 Epsilon=7 Iterations=200	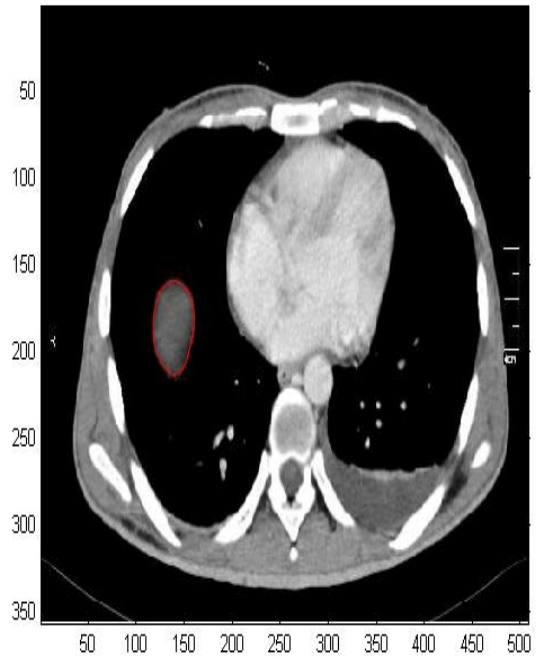

3	Alpha=1.5,3,3.5 Lambda=5,6,7 Epsilon=1.5,3 Iterations=100,150, 200	Alpha=-3 Lambda=7 Epsilon=7 Iterations=150	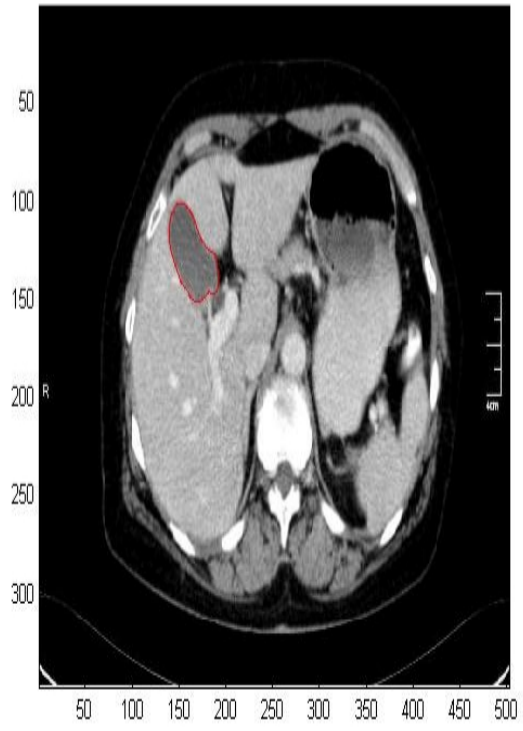
	Alpha=1.5,3,3.5 Lambda=5,6,7 Epsilon=1.5,3 Iterations=100,150 ,200	Alpha=-3 Lambda=7 Epsilon=7 Iterations=150	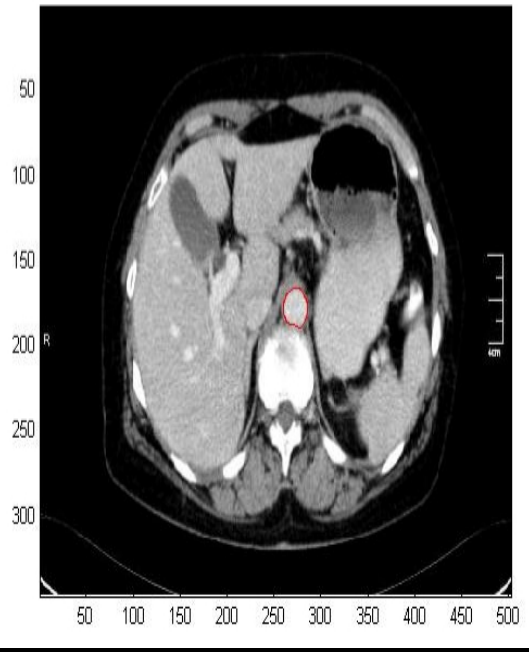

4	Alpha=1.5,3,3.5 Lambda=5,6,7 Epsilon=1.5,3 Iterations=100,150, 200	Alpha=-4 Lambda=7 Epsilon=7 Iterations=250	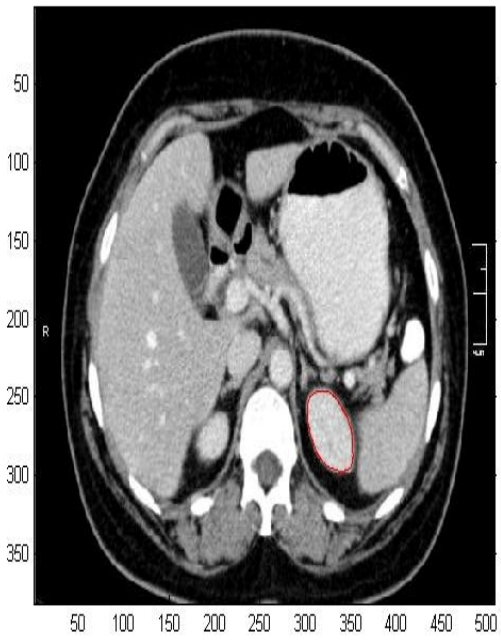
	Alpha=1.5,3,3.5 Lambda=5,6,7 Epsilon=1.5,3 Iterations=100,150, 200	Alpha=-3 Lambda=7 Epsilon=7 Iterations=150	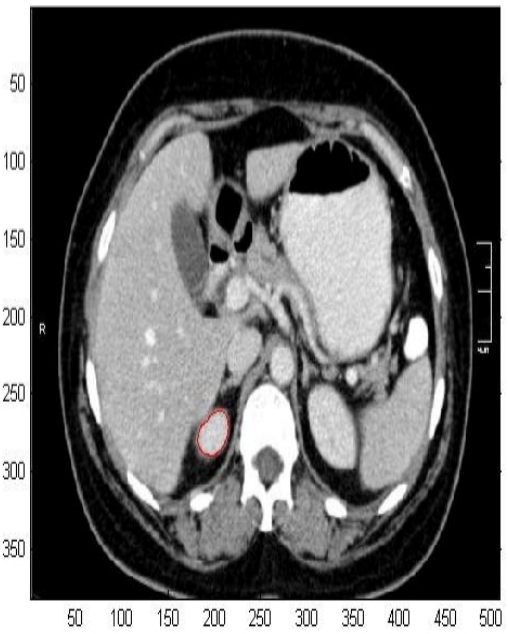

5	Alpha=1.5,3,3.5 Lambda=5,6,7 Epsilon=1.5,3 Iterations=100,150, 200	Alpha=-1.5 Lambda=7 Epsilon=7 Iterations=100	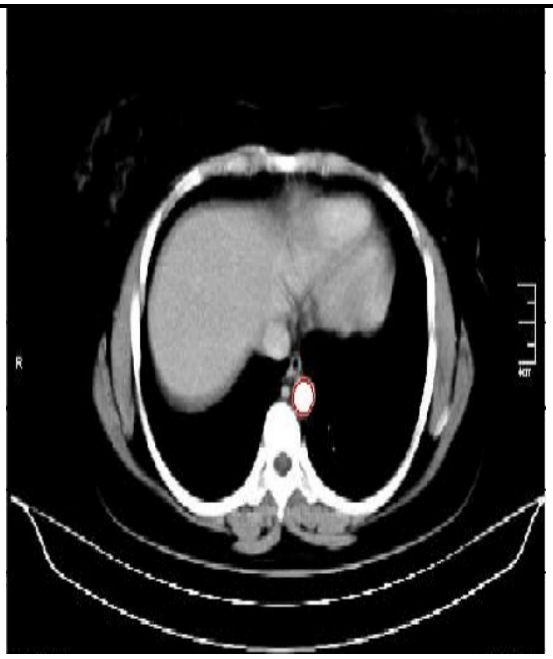
	Alpha=1.5,3,3.5 Lambda=5,6,7 Epsilon=1.5,3 Iterations=100,150, 200	Alpha=-1.5 Lambda=7 Epsilon=7 Iterations=100	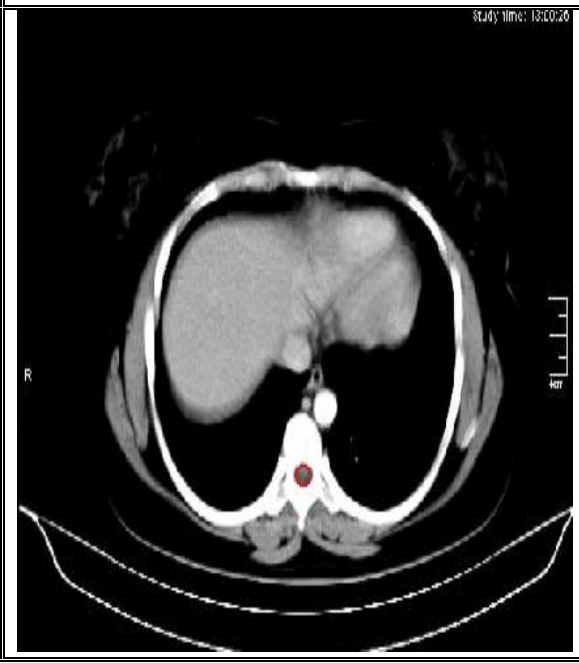

5.2.1 Different level-set parameters

Epsilon- The parameter in the definition of smoothed Dirac function refers equation 5.1, which is the responsible for the smoothing the level-set curve.

$$L_g(\phi) = \int_\Omega g\varepsilon(\phi)|\nabla\phi|dxdy \quad \text{.....5.1}$$

Time step- In implementing the proposed level set method, the time step τ can be chosen significantly larger than the time step used in the traditional level set methods. Using larger time step can speed up the evolution, but may cause error in the boundary location if the time step is chosen too large.. Usually, we use $\tau \leq 10.0$ for the most images.

Mu- It is the coefficient of the internal (penalizing) energy term P (ϕ) in the equations is given below. The product of time step and mu must be less than 0.25 for stability. It should be taken as

$$\mu = 0.2/\text{time step} \quad \text{.....5.2}$$

$$E(\phi) = \mu.p(\phi) + E_m \quad \text{.....5.3}$$

Lambda- Coefficient of the weighted length term Lg (ϕ), which is responsible for driving the zero level curve towards the object boundaries.

$$E_{g,}\ \lambda,\ \alpha\ (\phi) = \lambda L_g\ (\phi) + \alpha\ A_g\ (\phi) \quad \text{.....5.4}$$

Alpha- Coefficient of the weighted area term Ag (ϕ) in equation5.4, which can be positive or negative depending on the relative position of the initial level-set to the object of interest. For example, if the initial level-sets are placed outside the object, the coefficient α in the weighted area term should take positive value, so that the level-sets can shrink faster. If the initial level-sets are placed inside the object, the coefficient α should take negative value to speed up the expansion of the level-sets.

5.3 Selection of best texture feature

The entire feature does not support the logic on which we can make the rules for parameters. It should be varies according to the alpha, so that we can make the intervals for its selection. Like if contrast is less than 100 than alpha is equal to 1.5.in all texture parameters contrast and evaluated area is fall in this logic refer the table 5.3. For area we can simple say that if area is more than level-set take more time to segment and need more speed but technical speaking we has to consider contrast feature which also fall in this logic but less than the area. Form the fig 5.1 we can say that contrast at 1.5 value of alpha is low and start increasing. At value 3 of alpha it has more value and above four all other feature value get low but only contrast value is still increasing, means we can easily make the intervals on the basis of the value of alpha.

Table 5.3: Relation between alpha and all texture features

S.NO.	Alpha	Contrast	Area	Mean	Std	correlation	Energy	Homogeneity
1	3.5	360	1744	248	24	0.007	5.68E-04	0.127
1	3	143	586	199	33	0	0.0017	0.1706
2	3	111	706	194	38.14	0	0.0014	0.1844
2	3.5	372	1685	85.99	16.73	0	5.94E-04	0.1265
3	3	159	1629	117	15.18	0.6391	6.16E-04	0.1647
3	3	130	498	196.47	25.03	0	1.90E-03	0.1794
4	4	431	2122	194.85	27.28	0	4.70E-04	0.0746
4	3	194	821	184.29	35.54	0.003	1.20E-03	0.1534
5	1.5	89	307	24.02	22.6	0	3.20E-03	0.1318
5	1.5	35	146	104.54	20.87	0.0351	6.00E-03	0.2662

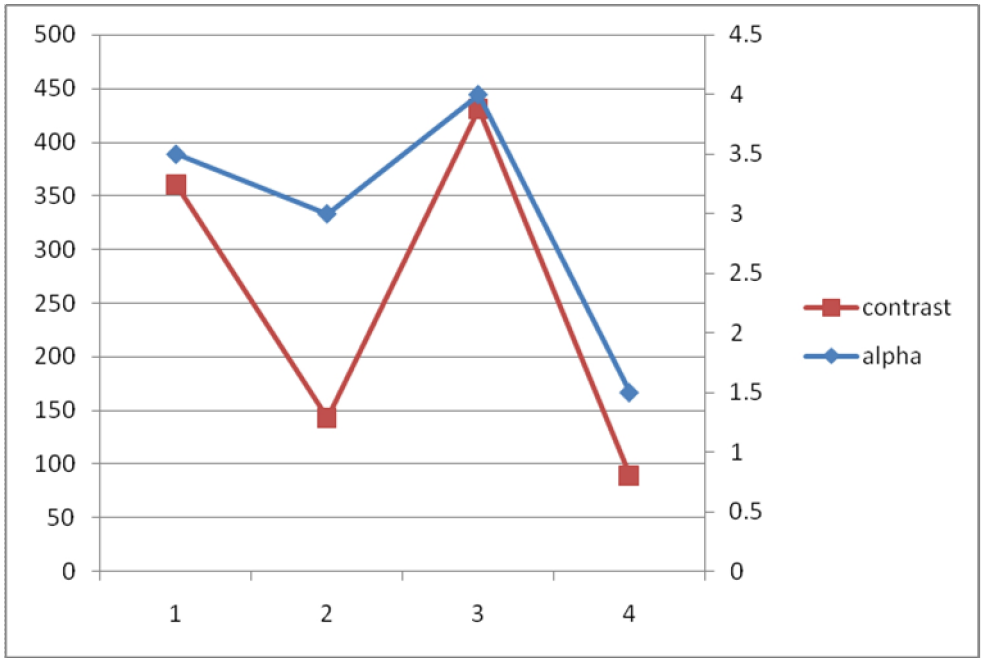

Fig 5.1: Comparison between alpha and contrast.

The relation between alpha and mean for all five images is shown in fig 5.2. Mean also show some linear relation with alpha at the starting of the curve, but at value three the mean starts decreasing and alpha start increasing.

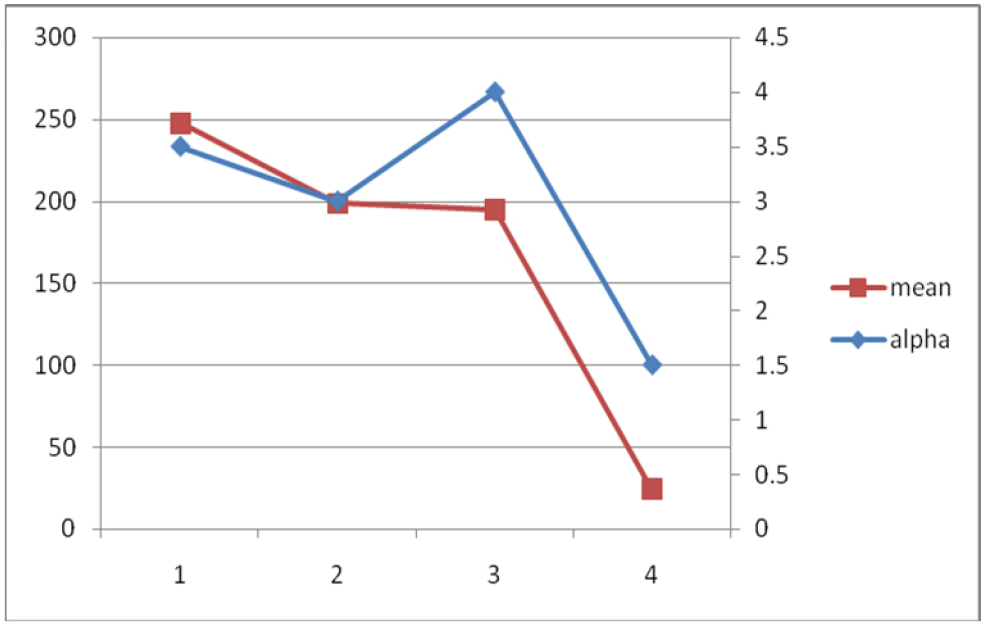

Fig 5.2: Comparison between alpha and mean.

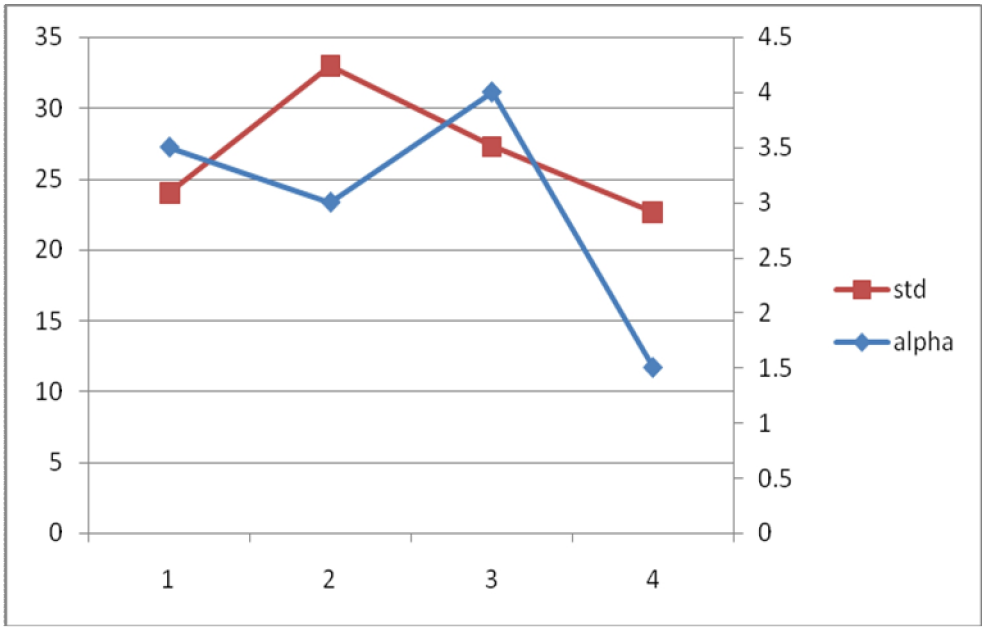

Fig 5.3: Comparison between alpha and standard deviation.

The fig 5.3 concludes that there is no any relation between alpha and standard deviation.

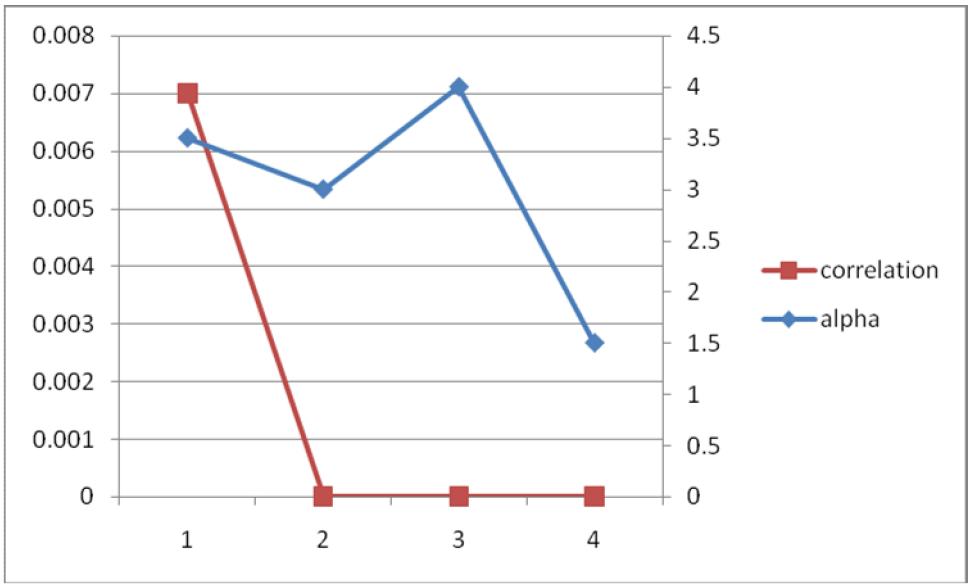

Fig 5.4: Comparison between alpha and correlation.

The fig 5.4 shows that the alpha parameter of the level set segmentation does not depend upon the correlation of the image.

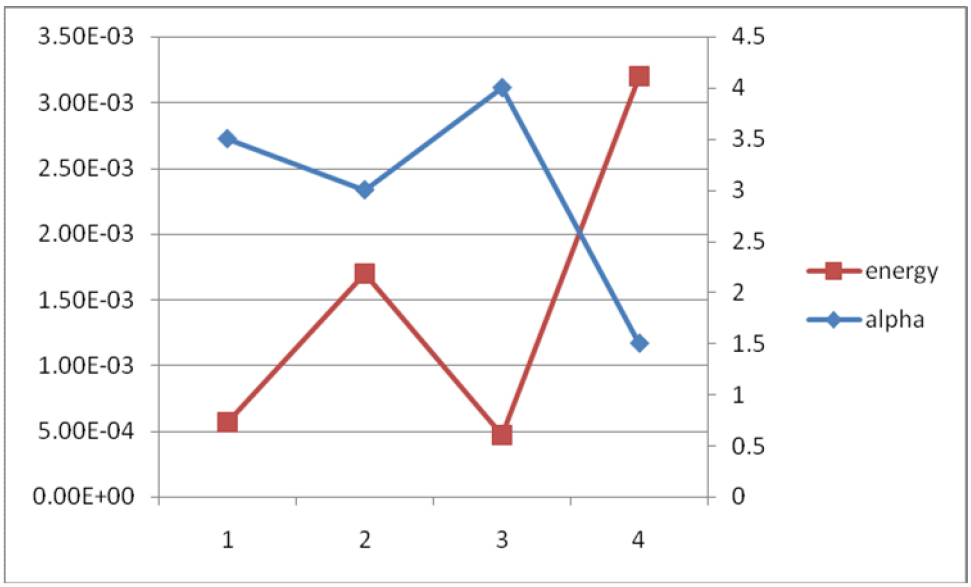

Fig 5.5: Comparison between alpha and energy.

The graph between energy and alpha is shown in fig. 5.5. It depict, the alpha value is independent of energy for images.

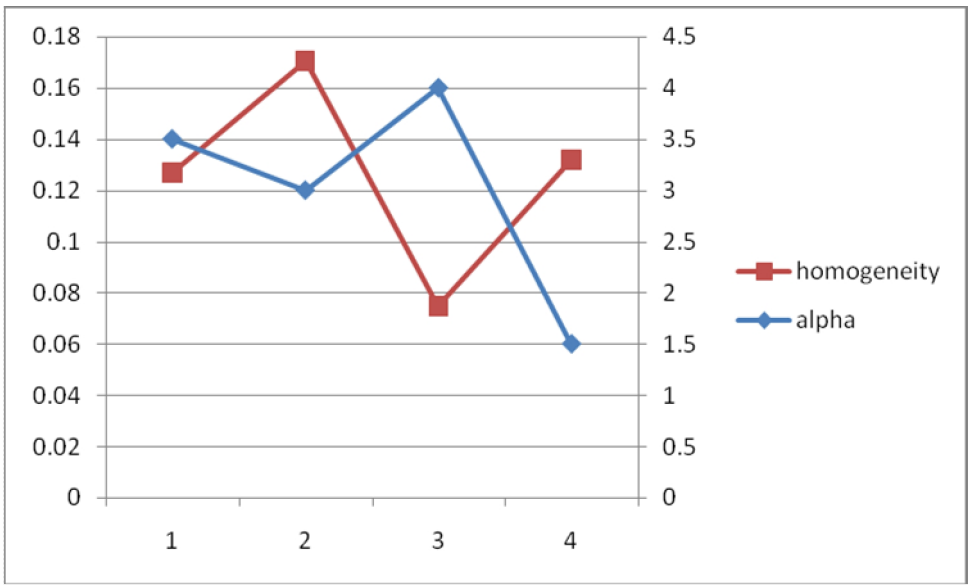

Fig 5.6: Comparison between alpha and homogeneity.

Homogeneity of the image is varying inversely with the alpha as shown in fig. 5.6. Homogeneity value cluster is more, because of that we does not use this feature for automatic segmentation of CT images.

5.4 Results of the segmentation program

All the three part of the program are joined and run it for segmentation. There is no need to do any tuning of the parameters of segmentation according to the contrast of the image. Parameter of the segmentation is automatically adjusted by the program itself for both data type either it is stored or not. The results are tested by the doctor of P.G.I; Chandigarh. The segmented images are shown in table 5.3.

Same images are used to test the code which segment the images depends upon another texture feature like mean of the image which shows some relation with alpha as shown in fig 5.2. This method does not segment all the images. Results are shown in table 5.4.

Table 5.4: Automatically optimized segmented images on the basis of contrast of the image

1	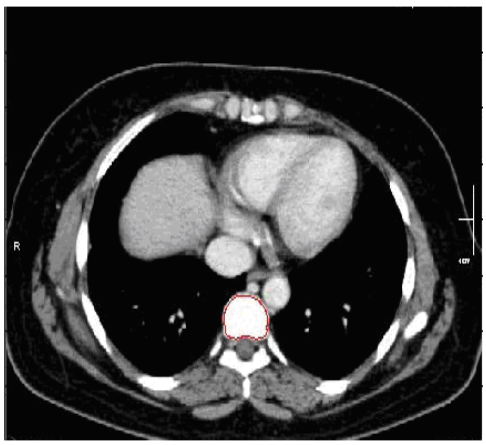	2	

3		4	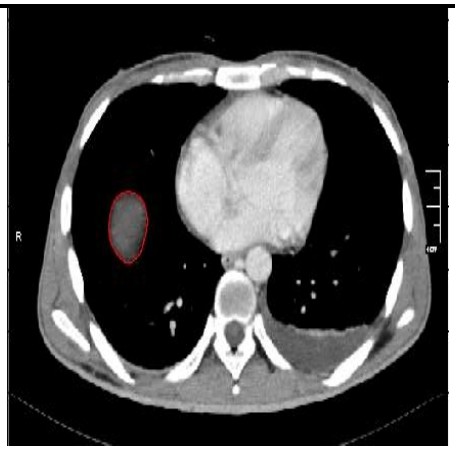
5	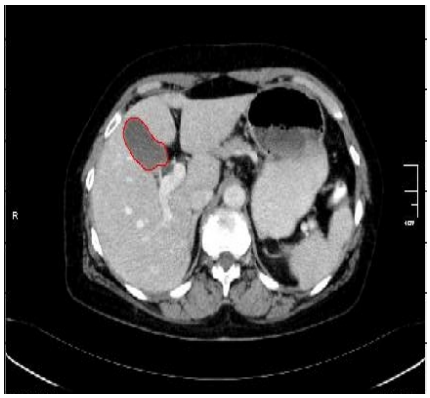	6	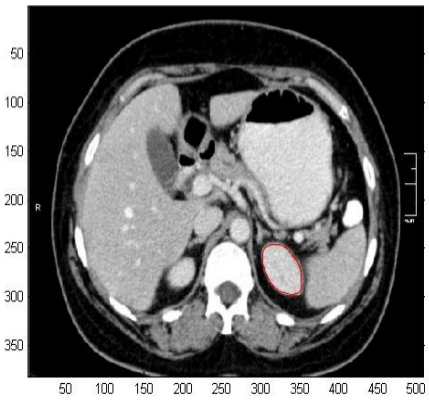

Table 5.5 Automatically optimized segmented images on the basis of mean of the image

1	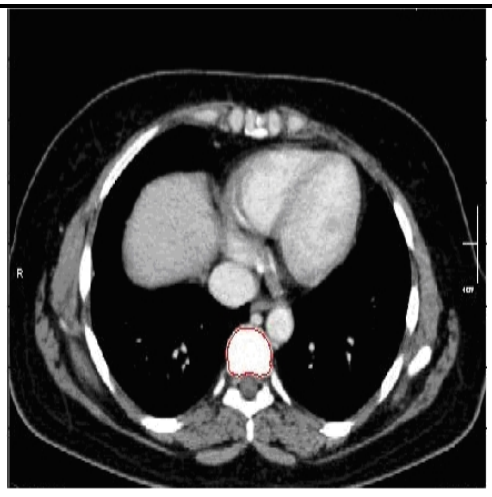	2	

3	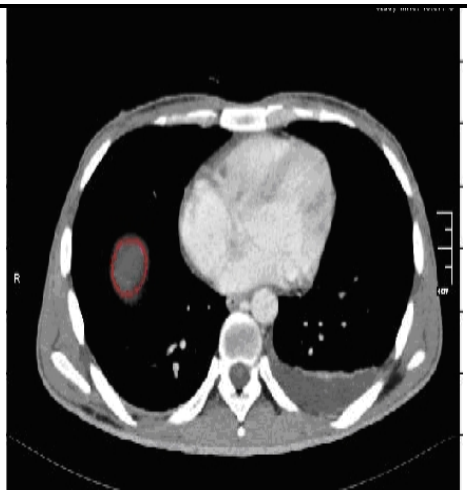	4	 DFOV 36.0cm STND kV 120 mA 270 Large 7.0 mm/1.5:1 Tilt : 0.0
5	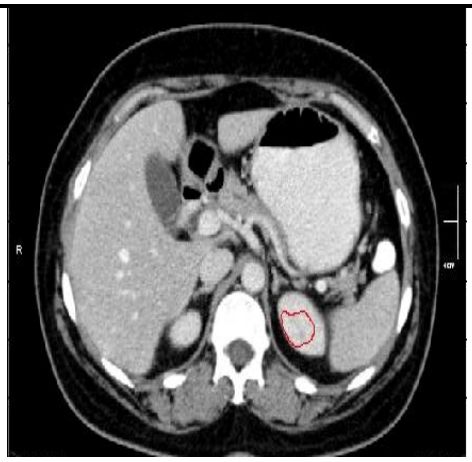	6	

5.5 CONCLUSION

This thesis provides the code for parameter optimization for segmenting structures in CT images, work likes an intelligent system. It segments the different CT images without tuning the level-set parameters and gives optimized results for all CT images. This code has different topology for segmentation and it automatically selects the optimized topology according to the given image.

5.6 SCOPE FOR FUTURE WORK

This thesis works only for CT images but in future it can be improved for different images like MRI, ultrasound and X-ray images. In this condition there is a requirement of proper selection of texture feature for images which depends upon the segmentation parameters. In case of large database fuzzy logic can be implemented for getting more accurate results.

References

[1] Chris.Davatzikos and Jerry.L.Prince "Adaptive Active Contour Algorithms for Extracting and Mapping Thick Curves" *IEEE Computer Society Conference on Computer Vision and Pattern Recognition*, 1993. page: 524 - 529

[2] C.T. Tsai Y.N. Sun P.C. Chung "Minimizing the energy of active contour model using a Hopfield Network." *IEEE Computers and Digital Techniques*, Nov 1993 Vol: 140, page: 297 – 303

[3] D.N.Davis, K.Natarajan and E.Claridge "Multiple Energy Function Active Contours Applied To CT And MR Images *IEEE International Conference on Image Processing and its Applications* Jul 1995 page: 114 – 118

[4] M. Xiao'. Y. Q. Shi2, D. Kris toll. L. Hom. P. Engler "Contour Extraction from HVEM image or Micro Vessel uisnf Active Contour models" *IEEE Proceedings of 20th Annual Northeast Bioengineering Conference, 1994.,* March 1994 page: 1 – 2

[5] Guillermo Sapiro "Vector-Valued Active Contours" *IEEE Computer Society Conference on Proceedings CVPR Computer Vision and Pattern Recognition* June 1996 page: 680 - 685

[6] Tianyun Ma and Hemant D. Tagare "Consistency and Stability of Active Contours with Euclidean and Non-Euclidea Arc Lengths"*, IEEE Transactions on Image Processing* Nov. 1999 Volume: 8 page: 1549 – 1559.

[7] F. Mendels, C. Heneghan, P. D. Harper, R. B. Reilly, and J.-Ph. Thiran "Extraction Of The Optic Disk Boundary In Digital Fundus Image." *Proceedings of the First Joint Conferenceof [Engineering in Medicine and Biology, 21st Annual Conf. and the Annual Fall Meeting of the Biomedical Engineering Soc.* Oct. 1999,Volume: 2, page: 1139 vol.2

[8] Yuki Matsuzawa and Toru Abe "Region Extraction Using Competition of Multiple Active Contour Models" *International Conference on Image Processing,* Oct. 1999,Volume: 3 page: 198 - 202

[9] Tony F. Chan and Luminita A. Vese "Active Contours Without Edges" I*EEE Transactions on Image Processing,* Feb. 2001,Volume: 10 , page: 266 – 277.

[10] Nilanjan Ray, Scott T. Acton, Talissa Alia2 and Eduard E. de Lunge " MRI Ventilation Analysis By Merging Parametric Active Contours" *International Conference on Image Processing,* Oct. 2001 Volume: 2, page: 861 - 864

[11] Di Xiao, Wan Sing Ng, Udantha R. Abeyratneb, Charles B. Tsang " Muscular Layer's Boundary Detection from Anal Ultrasound Image by Active Contour Method" *Seventh international Conference on Control, automation, Robotizes And Vision (ICARCV'OZ)*, Dec 2002,

[12] LJ Spreeuwers, M Breeuwer "Myocardial Boundary Extraction Using Coupled Active Contours" *IEEE Conference on Computers in Cardiology,* Sept. 2003 page: 745 - 748

[13] Ning Xu, Ravi Bansal & Narendra Ahuja "Object Segmentation Using Graph Cuts Based Active Contours" *IEEE Computer Society Conference on Computer Vision and Pattern Recognition,*2003 Volume: 2 page: II - 46-53.

[14] Peter.J.Yim & David.J.Foran "Volumetry of Hepatic Metastases in Computed Tomography using the Watershed and Active Contour Algorithms" *Proceedings of the 16th IEEE Symposium on Computer-Based Medical Systems*, June 2003 page: 329 - 335

[15] Lijun Yin, Sandeep Deshpande & Ja Kwei Chang "Automatic Lesion / Tumor Detection Using Intelligent Mesh-Based Active Contour" *Proceedings of the 15th IEEE International Conference on Tools with Artificial Intelligence (ICTAI'03)*, Nov. 2003 page: 390- 397

[16] Raquel Valdés-Cristerna "Coupling of Radial-Basis Network and ActiveContour Model for Multi-spectral Brain MRI Segmentation" *Ieee Transactions On Biomedical Engineering*, VOL. 51, NO. 3, MARCH 2004, page: 459 - 470

[17] Nilanjan Ray and Scott T. Acton "Motion Gradient Vector Flow: An External Force forTracking Rolling Leukocytes With Shape and SizeConstrained Active Contours" *IEEE Transactions On Medical Imaging*, VOL. 23, December 2004

[18] M. Savelonas, D. Maroulis, D. Iakovidis "A Variable Background Active Contour Model for Automatic Detection of Thyroid Nodules in Ultrasound Images." *IEEE International Conference on Image Processing,* Sept. 2005 Volume: 1 , page: I - 17-20

[19] Chunming Li, Chenyang Xu, Changfeng Gui, and Martin D. Fox,"Level Set Evolution Without Re-initialization: A New Variational Formulation" *IEEE Computer Society Conference on Computer Vision and Pattern Recognition,* June 2005 Volume: 1 page: 430 - 436

[20] Umasankar Kandaswamy "Efficient Texture Analysis of SAR Imagery", *IEEE Transactions on Geoscience and Remote Sensing,* Sept. 2005 Volume: 43, Issue: page: 2075 – 2083

[21] Suk-Ho Lee and Jin Keun Seo "Level Set-Based Bimodal Segmentation With Stationary Global Minimum" *IEEE Transactions on Image Processing,* Sept. 2006 Volume: 15 , page: 2843 – 2852

[22] folk.uio.no/runeps/studies/thesis-presentation2005.pdf

[23] en.wikipedia.org/wiki/Graphics_file_format.

[24] P.G.I chandigarh/radiology department/CT images (DICON images extract by k-pacs software)

[25] www.med.wayne.edu/diagradiology/Anatomy_Modules/Abdomen.html

[22] S. Osher, J. A. Sethian, "Fronts propagating with curvaturedependent speed: algorithms based on Hamilton-Jacobi formulations", *J. Comp. Phys.*, 1988, vol. 79,. pp. 12-49,

[23] The Handbook of Pattern Recognition and Computer Vision (2nd Edition), by C.H. Chen, L. F. Pau, P. S. P. Wang (eds.), *World Scientific Publishing Co.*, 1998. Chapter 2, pp. 207-248

[24] Arati S. Kurani, Dong-Hui Xu, Jacob Furst, Daniela Stan Raicu " co-occurrence matrices for volumetric data" *Journal of the American Society for Information Science and Technology* 2006 volume 57 , Issue 12 Pages: 1616 - 1628

[25] Image Segmentation by Texture Analysis by Cecilia Di Ruberto , Giuseppe Rodriguez, Sergio Vitulano 1999.

[26] www.mathworks.com/access/helpdesk/help/toolbox/images/index.html